

Progress Report for R&D Projects [Completion report]*

Section-A : Project Details

(This report contains only the technical part of the project. The detailed utilization/statement of expenditure will be sent separately)

A1. Project Title : Studies on the efficacy of flavonoid and non-flavonoid polyphenols against chronic inflammation induced disease pathogenesis.

A2. DBT Sanction Order No. & Date : BT/469/NE/TBP/2013 dt. 14/10/2015

A3. Name of Principal Investigator(s): Dr. Rupak Mukhopadhyay (Tezpur University) and Dr. Kaushik Biswas(Bose Institute, Kolkata)

Name of Co-PI/Co-Investigator: Prof. A. K. Mukherjee (Tezpur University) and Dr. Anup K. Misra (Bose Institute, Kolkata)

A4. Institute: Tezpur University, Assam and Bose Institute, Kolkata

A5. Address with Contact Nos. (Landline & Mobile) & Email :

Dr. Rupak Mukhopadhyay: Department of Molecular Biology and Biotechnology, Tezpur University, Assam 784028, Phone 03712-275417 (Off), 09954471591 (Mobile)

Dr. Kaushik Biswas: P1/12 C.I.T. Scheme VIIM, Division of Molecular Medicine, Bose Institute, Kolkata 700054, Phone : 033-25693217 (Off.), 9007191031 (Mobile)

A6. Total Cost (funds received): Rs. 76.37 lakhs (Rupees Seventy six lakhs thirty seven thousand only)

A7. Duration: 3 Years (03.03.2014 to 02.03.2017; Extended up to 02.09.2017)

A8. Approved Objectives of the Project:

- 1. To identify potential anti-inflammatory flavonoid and non-flavonoid polyphenols using cell culture studies*
- 2. To study selected compounds for anti-atherosclerotic and/or anti-cancer activities in vitro*
- 3. To determine the efficacy of 2-3 lead compounds in preventing chronic inflammation induced pathogenesis in animal models*
- 4. To generate derivatives of parent compounds by functional group modifications to enhance their anti-cancer and/or anti-atherosclerotic activity*

A9. Specific Recommendations made by the Task Force (if any): Not applicable

Section-B : Scientific and Technical Progress

PROJECT COMPLETION REPORT (Consolidated)

B1. Progress made against the Approved Objectives, Targets & Timelines during the Reporting Period (1000-1500 words for interim reports; 2500-3500 words for final report; data must be included in the form of up to 3 figures and/or tables for interim reports; up to 7 figures and/or tables for final reports).

Objective I: *To identify potential anti-inflammatory flavonoid and non-flavonoid polyphenols using cell culture studies*

Screening of polyphenols for their anti-inflammatory efficacy: Polyphenols namely Kaempferol, EGCG, Chrysin, Quercetin, Ferulic acid, Eriodictyol, Morin hydrate, Rutin hydrate, Ellagic acid, Hesperetin, Pyrogalllic acid, Apigenin (6 by Bose Institute, 6 by TU) were screened for their anti-inflammatory efficacy using lipopolysaccharide (LPS) as the inflammation-inducer. The polyphenols Genistein, Biochanin A, Myricetin, Daidzein, Pelargonidin chloride were screened using IL-6 as the inflammation-inducer (Figure 1) (at TU). The primary screening data has been shown in previous years' reports. Based on the result obtained, detailed study on anti-inflammatory mechanism of action was done on Kaempferol and Biochanin A. On the other hand, anti-inflammatory efficacy of Eriodictyol proved to be an excellent anti-cancer agent.

PMA-differentiated macrophage cell line THP-1 were pre-treated with the above-mentioned polyphenols (Biochanin A, Daidzein, Genistein, Pelargonidin chloride, Myricetin and Kaempferol) at different concentrations for specific time periods followed by IL-6 (50 ng/mL) for 2 hours. Eriodictyol, on the other hand was studied in LPS-induced THP-1 cells. Cells were harvested for RNA isolation followed by cDNA synthesis and PCR using gene-specific primers. Gene expression analysis of important pro-inflammatory mediators such as MCP1, IL-1 β , TNF- α COX-2 was done.

While all six polyphenols showed some activity, Biochanin A significantly inhibited MCP1, IL-1 β , IL-34, IL-17 dose-dependently but modulated TNF- α , ICAM-1 only at higher concentrations used, while it did not have a profound inhibitory effect on CCR2-A (Figure 1E). Similarly, Kaempferol and Eriodictyol also showed significant anti-inflammatory activity (Figure 1F and 1G). The differential inhibitory effect of Biochanin A on the various inflammatory mediators checked, intrigued us to study its anti-inflammatory mechanism of action upon IL-6 induction in a detailed manner. Moreover, till date, no study has been done on the effect as well as mechanism of action of Kaempferol and Biochanin A on IL-6-induced macrophages. Since not much is known regarding the anti-cancer efficacy of eriodictyol, compared to other anti-inflammatory compounds screened, we explored the possible anti-cancer efficacy of eriodictyol in various cell culture models as a part of Objective 2.

Figure 1

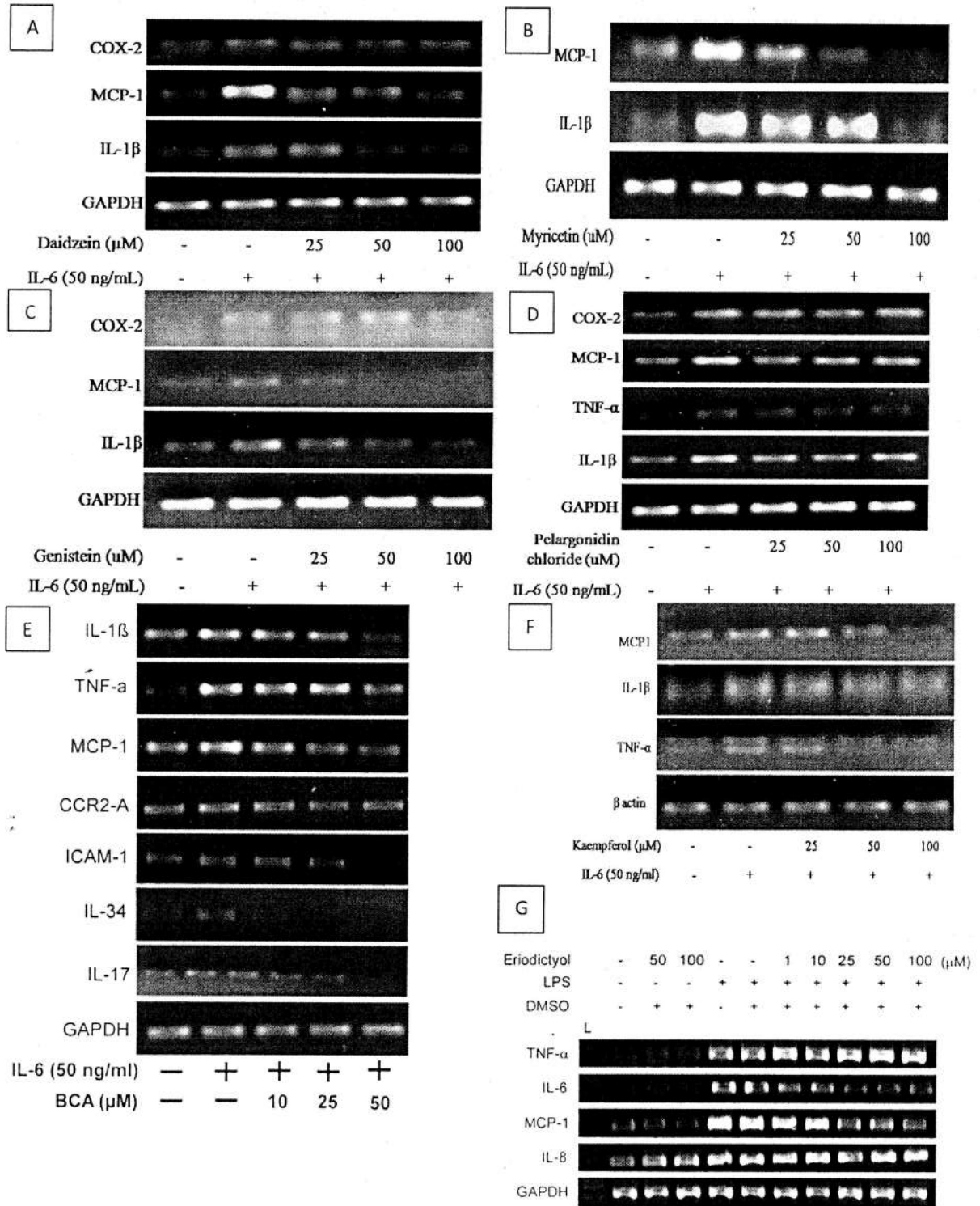


Figure 1: Anti-inflammatory efficacy of the polyphenols Daidzein (A), Myricetin (B), Genistein (C), Pelargonidin chloride (D), Biochanin A (E) and Kaempferol (F) in IL-6 (50 ng/mL)-induced and Eriodictyol (G) in LPS-induced THP1 macrophages. Semi-quantitative PCR using gene-specific primers of pro-inflammatory mediators was performed.

Objective 2. To study selected compounds for anti-atherosclerotic and/or anti-cancer activities in vitro

Anti-inflammatory efficacy of kaempferol: We have shown the potent anti-inflammatory efficacy of kaempferol by its ability to inhibit the expression of important pro-inflammatory mediators, IL-1 β , COX-2, TNF- α , MCP-1 in both LPS as well as IL-6 induced THP1 cells. Several studies elucidated kaempferol-mediated attenuation of LPS-mediated inflammation [1-4]. But other than bacterial infections, the body has to fight inflammation caused by its own cytokines, such as IL-6, TNF- α , MCP-1, etc. Interleukin 6 (IL-6) is a pleiotropic cytokine that exhibits either a pro- or an anti-inflammatory effect in diverse cell types and conditions [5-7]. We compared the effect of kaempferol on three important transcription factors such as, NF-kB, STAT3, ERK p42/44. In case of LPS induction, the polyphenol inhibited activation of all three transcription factors (Figure 2A); however, in IL-6-induced THP1 kaempferol significantly inhibited NF-kB and STAT3 but not ERK (Figure 2B). Differential inhibition pattern of transcription factors by kaempferol demanded further study. A detailed mechanistic study of kaempferol action on the expression of one of the major inflammatory mediator COX-2 has been carried out. COX-2 are known to contribute a great deal to inflammation-related disease pathogenesis such as rheumatoid arthritis, psoriasis, osteoporosis [8-13].

Figure 2

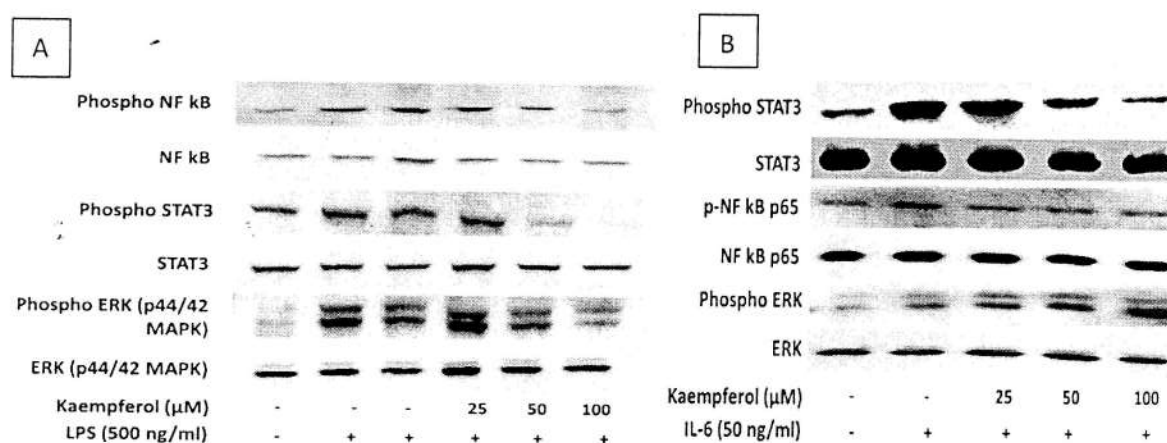


Figure 2: Western blot analysis suggesting kaempferol-mediated inhibition of NF-kB p65 (Ser 536), STAT3 (Tyr 705) and ERK p42/44 (Tyr 202-204) activation in LPS and IL-6-induced THP1 in a dose-dependent manner

Kaempferol attenuates COX-2 expression in IL-6-induced THP1 cells by modulating the activation of both STAT3 and NF-kB: Cyclooxygenase-2 (COX-2) is one of the key enzymes that catalyzes the conversion of arachidonic acid to inflammatory mediators, prostaglandins and prostanoids [14-16]. We showed for the first time, that kaempferol inhibits IL-6-induced expression of COX-2, an important pro-inflammatory mediator, at both mRNA and protein level,

in THP1 macrophages (Figure 3 A, B).As shown above, we also found that kaempferol prevents the activation of the two important transcription factors, STAT3 and NF-kB, in IL-6-induced THP1.

Figure 3

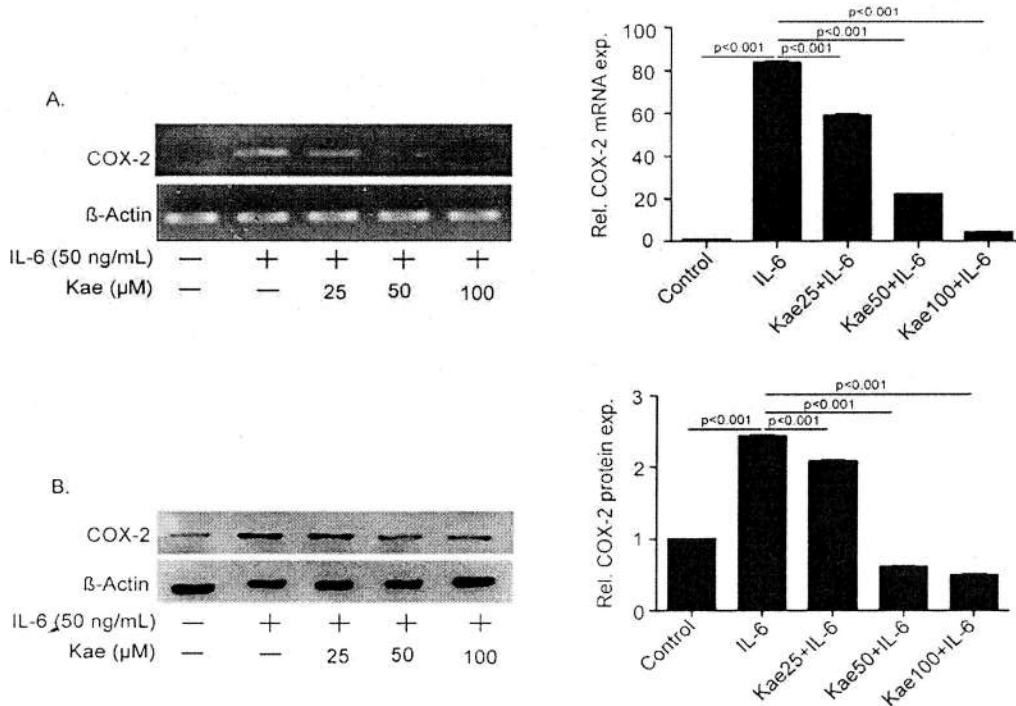


Figure 3: Kaempferol attenuates the mRNA and protein expression of COX-2 in IL-6-induced THP1. Semi-quantitative PCR using COX2-specific primer (A) and western blot analysis (B) using anti-COX-2 monoclonal antibody (Clone D5H5) were performed in THP-1 cells induced with various doses of IL-6.

STAT3 is known to be the major transcription factor in IL-6 signaling [17-19], however its role in controlling COX-2 expression in macrophages and how kaempferol prevents this phenomenon is not known. Moreover, NF-kB is known to be the major factor that regulates COX-2 upon induction with other inducers such as LPS [20, 21]. But the effect of NF-kB, in IL-6 induced expression of COX-2 in macrophages is yet to be reported. Towards this goal, we tried to elucidate the role of both STAT3 and NF-kB in IL-6-induced COX-2 expression in our model. We individually inhibited STAT3 and NF-kB using specific inhibitors to see their respective effect on COX-2 expression in the given system.

PMA-differentiated THP1 macrophages were pre-treated with the STAT3 inhibitor S3I-201 (500 μ M) for 15 min followed by IL-6 induction for 2 h. Western blot analysis showed that COX-2 expression was reduced as compared to IL-6-induced sample upon STAT3 inhibition. In addition, pre-treatment with both kaempferol (100 μ M) and S3I-201 (500 μ M) further reduced

COX-2 expression to many folds, suggesting another pathway in addition to JAK-STAT pathway for IL-6-induced COX-2 expression (Figure 4A).

Next, we inhibited NF- κ B activation to elucidate its role in IL-6-induced COX-2 expression. Pre-treatment with the NF- κ B inhibitor, Bay-11 (20 μ M) for 1 h followed by IL-6 induction reduced COX-2 expression significantly (Figure 4B). This suggested that NF- κ B is playing a major role in addition to STAT3 for the expression of COX-2 upon IL-6 induction in macrophages. This finding confirms that kaempferol inhibits IL-6-induced COX-2 expression by inhibiting the activation of both STAT3 and NF- κ B.

Figure 4

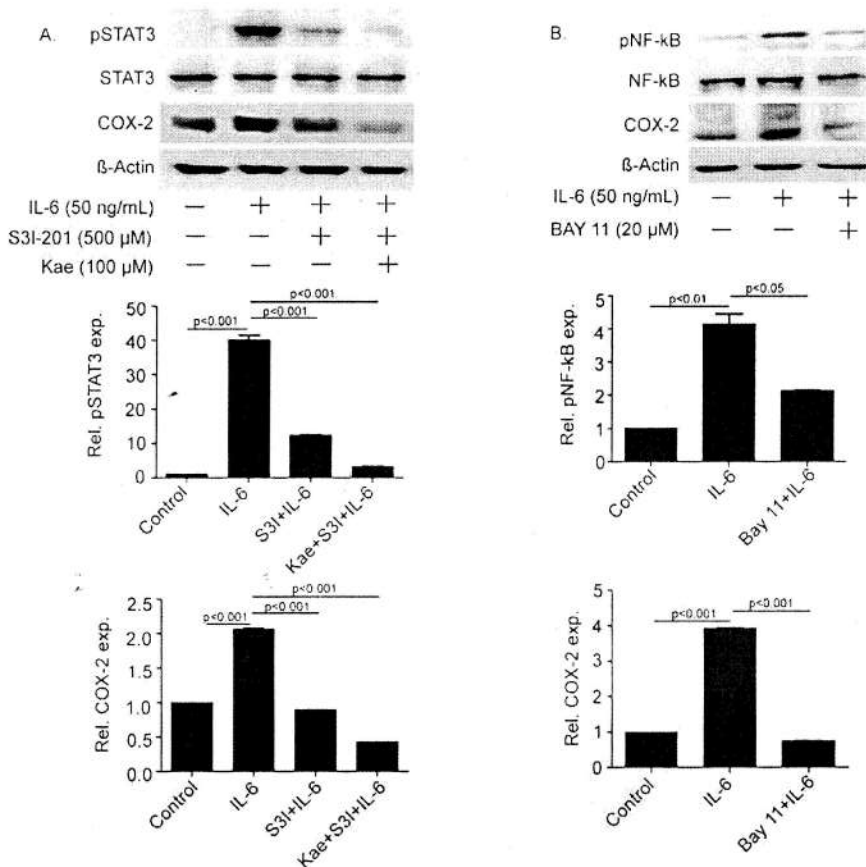


Figure 4: STAT3 and NF- κ B activation is required for IL-6 induced COX-2 expression. THP-1 cells were pre-treated with S31-201 alone or in combination with kaempferol (Kae) followed by induction with IL-6 (A). The cells were pre-treated with BAY-11 (B) before induction with IL-6. Expressions of p-STAT3 (Tyr 705), STAT3, p-NF- κ B (Ser536), NF- κ B and COX-2 were studied by western blots.

Kaempferol inhibits the nuclear translocation of p-STAT3 and NF- κ B p65: We further found that in addition to modulating the activation status of these two transcription factors, kaempferol also inhibits the nuclear localization of STAT3 and NF- κ B, hence preventing downstream

expression of COX-2. PMA-differentiated THP1 macrophages were pre-treated with kaempferol at two different concentrations (50 and 100 μ M) for 6 hours followed by IL-6-induction (50 ng/mL) for 2 hours. Immunostaining using antibodies specific to p-STAT3 (Tyr 705) and NF- κ B p65 (Ser 536) showed that increased translocation of these two transcription factors in the IL-6-induced sample was subsequently reduced dose-dependently in the kaempferol+IL-6 treated samples (Figure 5 A, B).

Figure 5

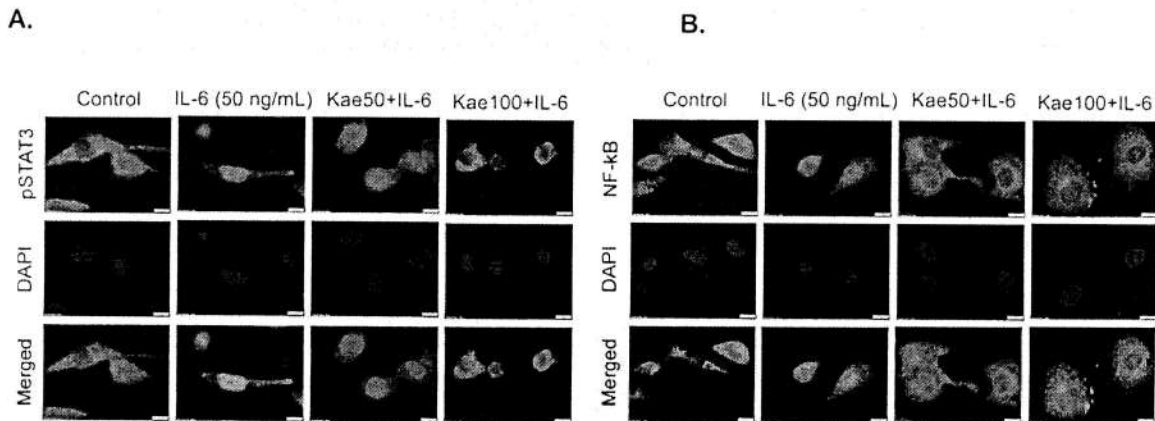


Figure 5: Kaempferol inhibits the nuclear translocation of IL-6-induced p-STAT3 and NF- κ B p65 in IL-6-induced THP1. Immunofluorescence images were taken using specific antibodies to study the effect of two different concentrations of kaempferol (50 and 100 μ M) treatment on nuclear translocation of p-STAT3 (A) and NF- κ B p65 (B).

Molecular Docking studies of kaempferol with STAT3 and NF- κ B: To understand the binding affinity of kaempferol with NF- κ B and STAT3, docking analysis was performed using Patchdock server (Figure 6A, B and Table 1). From our findings, we observed strong binding affinity and transient interaction in both NF- κ B/Kae and STAT3/Kae complexes. We noticed negative atomic contact energy and greater interface area for both the complexes. Selected complexes obtained from Patchdock were refined using Firedock online server which also suggested similar negative binding energy profile (Figure 6C). It is plausible that kaempferol attenuates COX-2 expression by directly binding to both STAT3 and NF- κ B proteins and inhibiting their activation and nuclear translocation.

Table 1: PatchDock results for the docking analysis of Kaempferol (Kae) with NF- κ B and STAT3

Complex	Solution	Geometric shape complementarity Score	Interface Area (\AA^2)	Atomic Contact Energy (kcal/mol)
NF-KAPPA B/Kae	3	3764	475.10	-229.11
STAT3/Kae	12	3566	478.80	-229.25

Figure 6

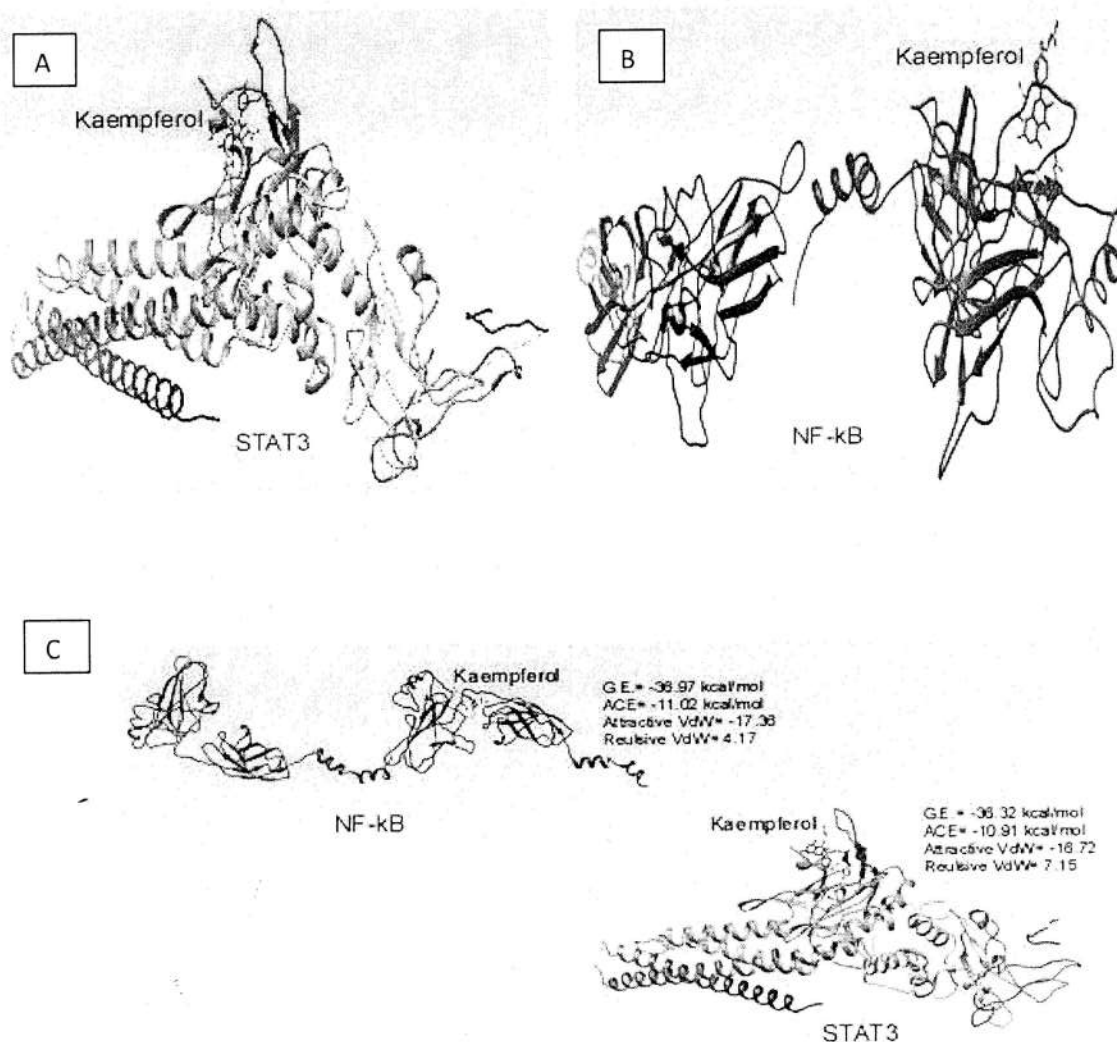


Figure 6: Docking analysis of kaempferol with STAT3 and NF-kB using Patchdock server (A, B). Refined docking analysis of kaempferol with NF-kB and STAT3 using Firedock server (C).

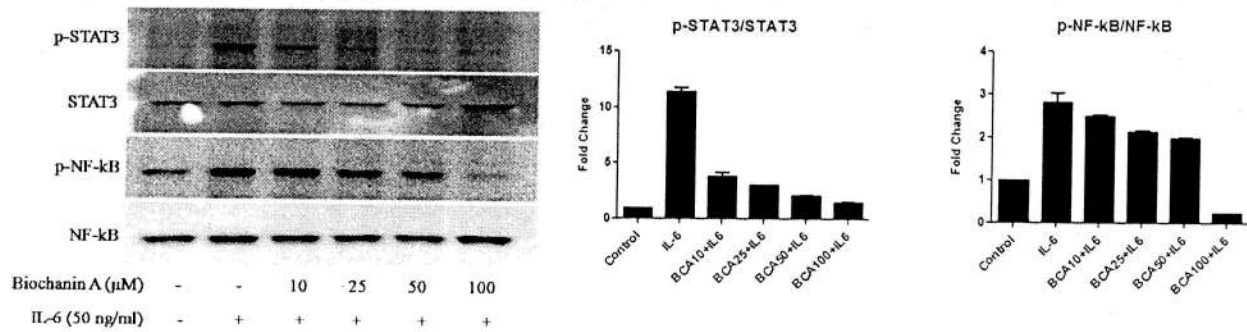
Mechanism of Anti-inflammatory efficacy of Biochanin A

Biochanin A was selected as the second polyphenol to be studied in detail for its mechanism of anti-inflammatory activity based on the result described in Figure 1. To understand the effect of Biochanin A on IL-6-induced THP-1 cells, western blot analysis of important transcription factors, namely, STAT3, NF-kB, ERK p42/44, p38 MAPK was performed. While Biochanin A successfully inhibited the activation of STAT3 dose-dependently, the activation of NF-kB p65 was decreased only at a higher concentration of Biochanin A (100 μ M) used (Figure 7A). When a viability assay with Biochanin A was performed, it was found that at 100 μ M concentration, 60% cells are viable (data not shown), which might be the reason of the sudden decrease of NF-

kB activation. On contrary, BCA increased the activation of ERK and p38 MAPK. While the phosphorylation of ERK p42/44 increased at 10 and 25 μ M, the activation of p38 MAPK was seen to increase from 10 upto 50 μ M of BCA used. BCA showed no effect on the third member of the MAPK family, *i.e.* p-JNK (Figure 7B).

Figure 7

A.



B.

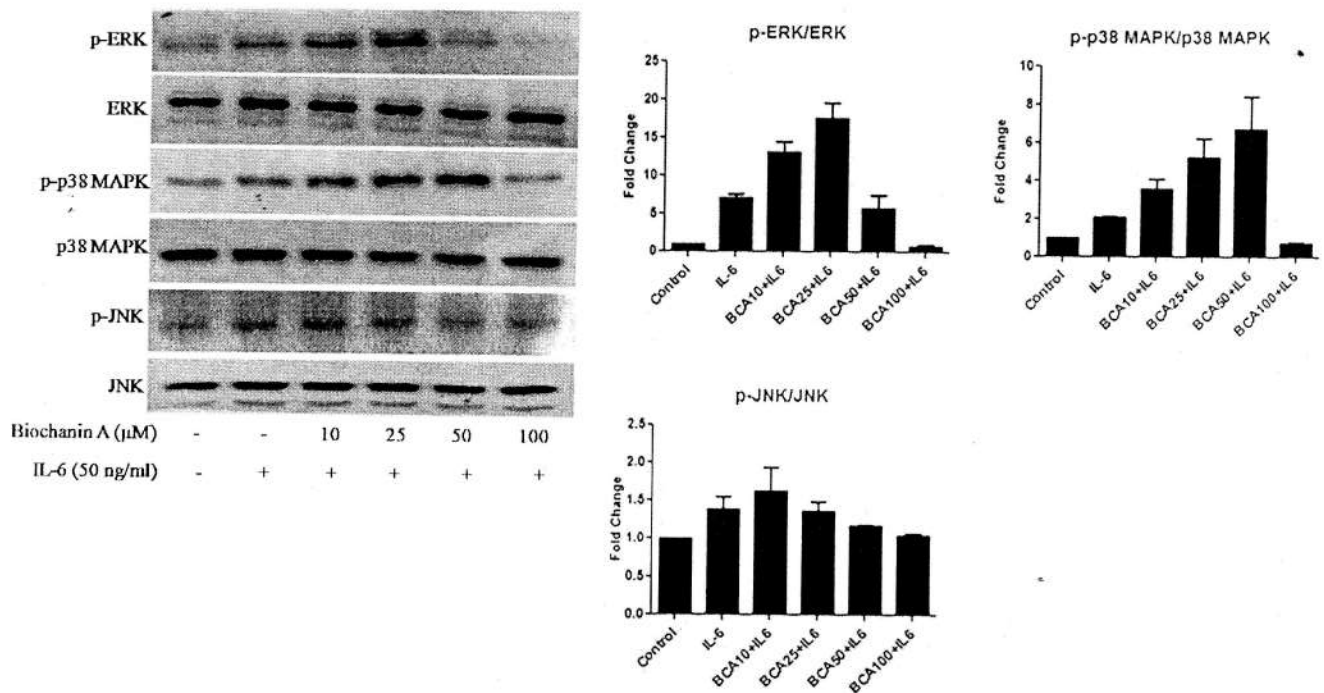


Figure 7: Biochanin A inhibits the activation of IL-6-induced STAT3 (Tyr 705) dose-dependently while it inhibits NF-kB phosphorylation only at a higher concentration (100 μ M) (A). Biochanin A increases the activation of IL-6-induced ERK and p38 MAPK at specific doses, while has no effect on JNK phosphorylation (B).

Reports suggested that MAPK might be a negative regulator of STAT3 in certain conditions [22-24]. Hence, we speculate that MAPKs might play a similar role in IL-6-induced and BCA-pre-treated cells; *i.e.* BCA might modulate STAT3 activation by increasing the activation of the MAPK's, ERK and p38 MAPK.

To study our hypothesis, we inhibited p38 MAPK with its specific inhibitor, SB203580 (CST, USA) at concentration of 50 μ M for 2 hours. We treated the cells with BCA (50 μ M) for 2 hours prior to MAPK inhibition. Finally, the cells were induced with IL-6 (50 ng/mL) for 2 hours. IL-6 treated cells and cells pre-treated with SB203580 followed by IL-6 induction were maintained as controls. After the treatments, cells were harvested for western blot analysis using specific antibodies to p-p38 MAPK as well as p-STAT3. Their non-phosphorylated forms were checked to ensure equal loading in all the wells while β -actin was used as the endogenous control. Phosphorylation of STAT3 was reduced in the SB203580+IL-6 sample but very significantly in BCA+IL-6 and BCA+SB203580+IL-6 samples (Figure 8). This result indicates that BCA inhibits STAT3 activation by enhancing the phosphorylation of p38 MAPK which in turn is negatively regulating STAT3 activation. However, further studies are necessary for its validation.

Figure 8

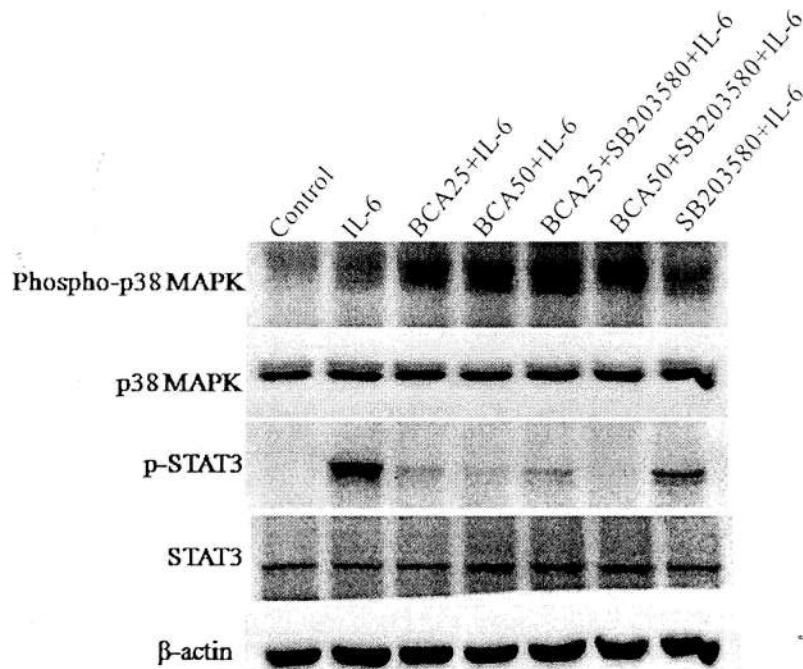


Figure 8: Biochanin A inhibits STAT3 activation by increasing p38 MAPK phosphorylation

Biochanin A prevents the nuclear translocation of p-STAT3: After understanding the role of BCA in inhibition of STAT3 activity, we were keen to understand the effect of BCA on the nuclear translocation of activated STAT3. Differentiated THP1 macrophages were pre-treated with 25 and 50 μM BCA for 2 hours followed by IL-6 (50 ng/mL) induction for 2 hours. Immunostaining was performed using antibody specific to p-STAT3 (Tyr 705) while nucleus was stained with DAPI. Results show that BCA prevents the nuclear translocation of p-STAT3 in a dose-dependent manner (Figure 9).

Figure 9

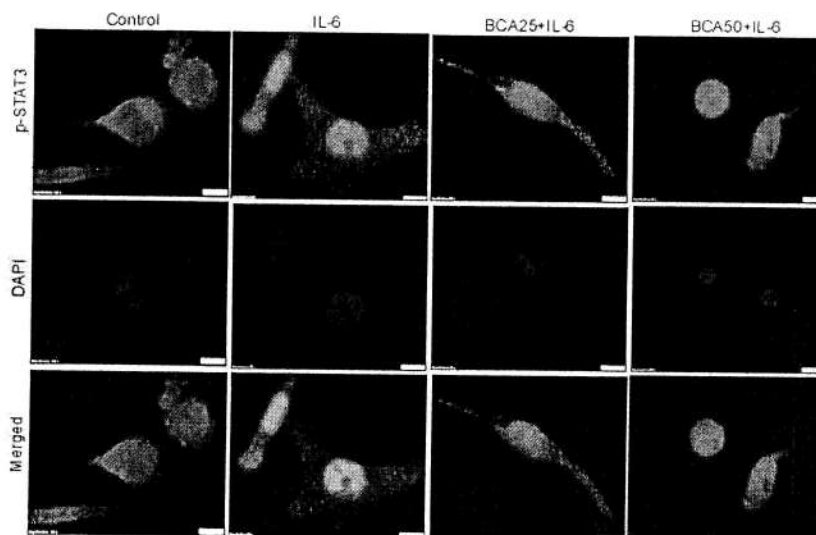


Figure 9: Biochanin A inhibits the nuclear translocation of IL-6-induced p-STAT3 in IL-6-induced THP1. Immunofluorescence images were taken using specific antibody to p-STAT3 (Tyr 705) to study the effect of two different concentrations of kaempferol (50 and 100 μM) treatment on nuclear translocation of p-

Biochanin A inhibits IL-6-mediated migration of THP1 cells: Migration is an important physiological function of monocytes to the site of inflammation. Hence, we were interested to study the effect of Biochanin A on the migration of THP1 cells upon IL-6 induction. Using Transwell 24-well plate (pore size, 5 μm), (Corning, USA), 0.1×10^6 cells/well were seeded in the lower chambers and differentiated with PMA (5 ng/mL). The THP1 macrophages were treated with Biochanin A (25 and 50 μM) for 2 hours followed by induction with IL-6 (50 ng/mL) for 2 more hours. Another well was treated with S3I-201 (500 μM) for 15 minutes followed by IL-6 treatment. All treatments were done in 1% serum-containing RPMI medium. After all the treatments, the treated cells were washed with PBS, replenished with serum-free medium and allowed to rest for 24 hours. After rest, approximately 0.1×10^6 THP1 monocytes (200 μL /well of serum-free medium) were seeded on the upper chambers and allowed for migration for 24 h at 37 $^\circ\text{C}$ in 5% CO_2 . Then the cells were fixed with 3.7% paraformaldehyde for 2-3 minutes followed by washing with PBS. Later, the cells were permeabilized using 100% methanol for 20 minutes

at room temperature and washed again with PBS. Finally, cells were stained with 0.05% crystal violet in PBS for 15 minutes. Cells on the upper side of the filters were removed with cotton swabs, while the lower sides were examined, imaged and counted under a microscope.

IL-6-induced migration of THP1 cells was subsequently reduced in the Biochanin A+IL-6 treated samples as well as the S3I-201+IL-6 treated samples as compared to only IL-6 treated sample (Figure 10). This implies that Biochanin A mediates the inhibition of IL-6-induced migration of THP1 by blocking STAT3 phosphorylation.

Figure 10

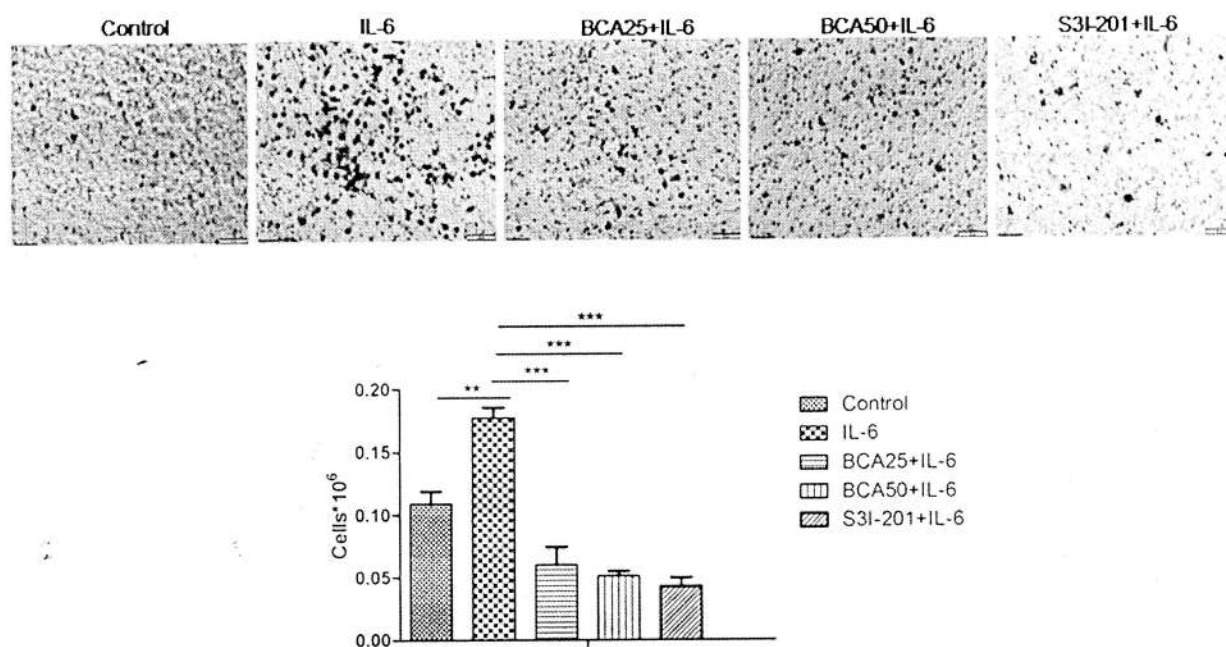


Figure 10: Effect of Biochanin A on IL-6-induced migration of THP1 monocytes

Biochanin A inhibits IL-6-mediated adhesion of THP1 cells: Similar to migration, adhesion is another important phenomenon occurring at the site of inflammation. An adhesion assay was performed to study the inhibitory effect of Biochanin A on the adhering property of THP1 cells upon IL-6 induction. 0.5×10^6 cells/well were seeded in a 6-well plate. Cells were pre-treated with BCA at 25 and 50 μ M concentration for 2 hours followed by IL-6 (50 ng/mL) for 2 hours. All treatments were done in 1% serum-containing RPMI medium. Thereafter, the cells were collected by centrifugation, washed and suspended in incomplete RPMI medium. In the meantime, polystyrene 96-well flat-bottomed microtiter plate (Nunc, Thermo Fisher Scientific, USA) was coated with 40 μ g/mL collagen Type I (Sigma-Aldrich, USA) (75 μ L/well) and dried.

100 μ L suspension of the treated cells were given in the collagen-coated wells and allowed to adhere for 1 hour in the CO₂ incubator. After 1 hour, media was removed and 100 μ L of 5% glutaraldehyde was given to each well and incubated for 20-30 minutes at room temperature. Wells were washed thrice with distilled water. The wells were stained with 100 μ L 2% crystal violet (Himedia, India) for 5 minutes. The cells were washed thrice with water and images were taken under microscope (Olympus). Then the stain was solubilized using 10% acetic acid and absorbance taken at 580 nm.

Samples treated with BCA+IL-6 and those treated with S3I-201+IL-6 showed lower adherence as compared to the IL-6-treated sample (Figure 11) which indicates that the phenomenon by which BCA is inhibiting adherence of THP1 cells is dependent on modulation of p-STAT3.

Figure 11

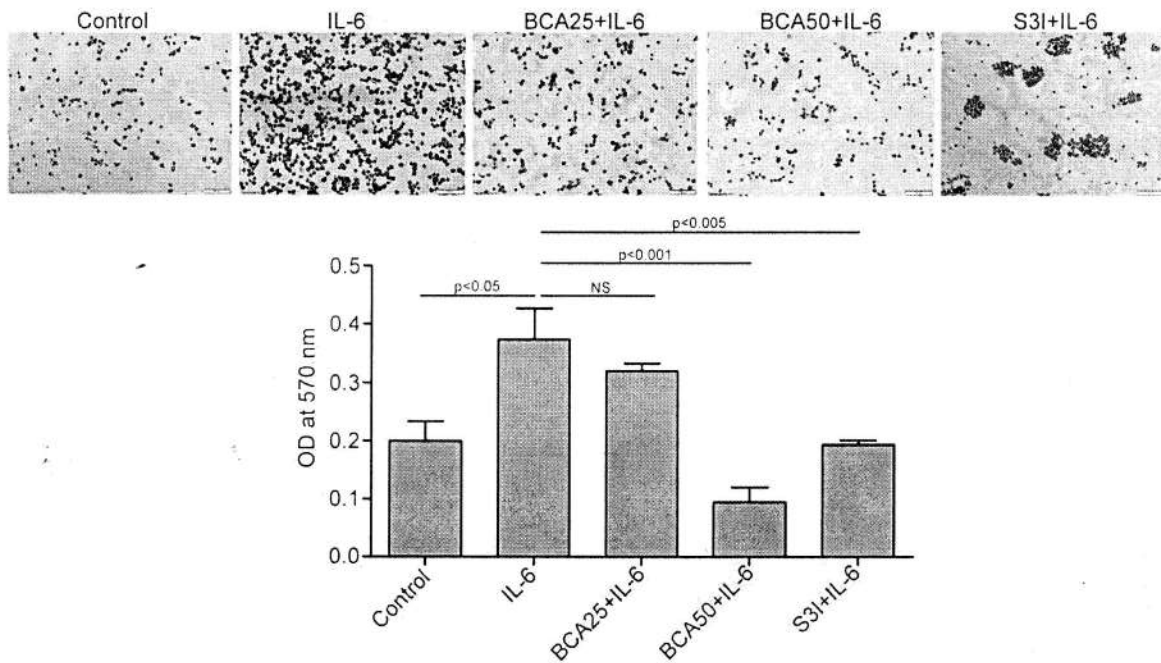


Figure 11: Effect of Biochanin A on the adhesion of THP1 monocytes upon IL-6 induction.

Mechanistic details of anti-cancer efficacy of Eriodictyol

Eriodictyol demonstrates selective cytotoxicity to cancer cells compared to normal cells: To assess the anti-proliferative activity of eriodictyol in tumor cell lines SK-RC-45 and HeLa versus normal cells, NKE and WI-38 cell line, 1×10^4 cells were seeded in 48 well plate format for 24 hrs in 300 μ l of complete RPMI-1640 media and incubated at 37 $^{\circ}$ C in presence of 5% CO $_2$. After 24 hrs, media was discarded and cells were treated with 25 - 200 μ M dose of eriodictyol for 48 and 72 hrs following which MTT at 0.5 mg/ml (dissolved in phenol red free media) was added and incubated for 3 hrs. The resulting intracellular purple formazan was solubilized in DMSO and quantified by spectrophotometry at 570nm. Results clearly show a significant dose and time-dependent decrease in viability of the tumor cells SK-RC-45 (Fig. 12c) and HeLa (Fig. 12d) in response to eriodictyol treatment with IC $_{50}$ values of 128 μ M and 95 μ M respectively. Compared to the tumor cell lines, eriodictyol did not show any significant effect on cell viability on the normal cells, WI-38 (IC $_{50}$ value > 200 μ M, Fig. 12a) or NKE cell line (IC $_{50}$ value >200 μ M, Fig. 12b). These data indicate a selective cytotoxicity of eriodictyol towards cancer cells compared to normal cells.

Figure 12

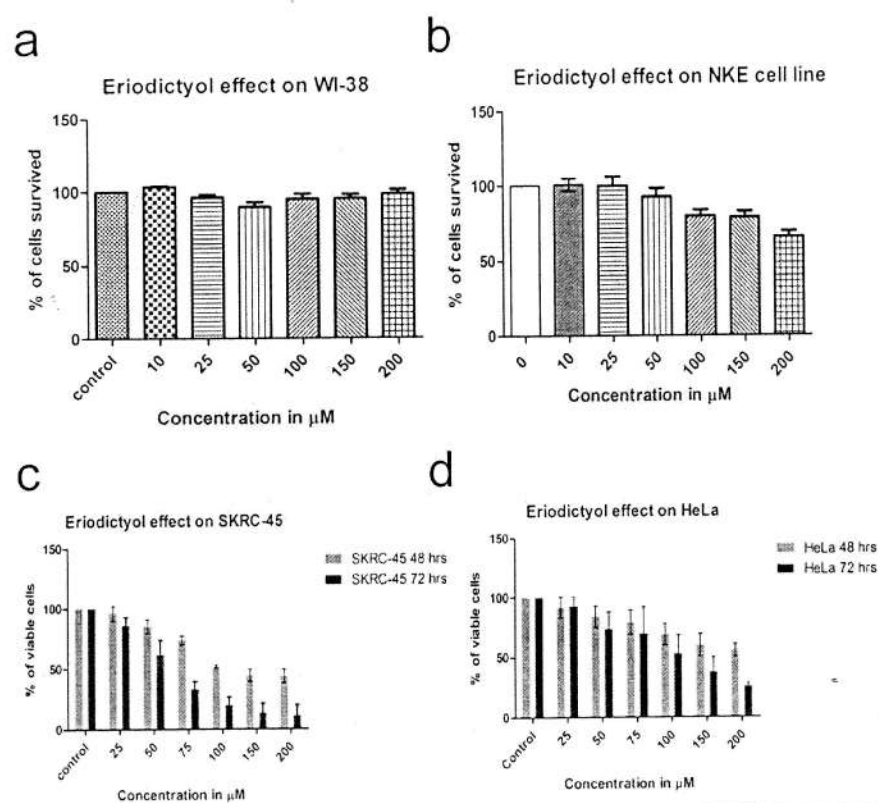


Fig. 12. Selective cytotoxicity of eriodictyol in human cancer cell lines versus normal cells. The ability of eriodictyol to block proliferation of human cancer cell lines, SK-RC-45 (c) and HeLa (d) were compared to those of normal cells, WI-38 (a) and NKE (b) by MTT. Ability of eriodictyol to block proliferation of cancer cells, SK-RC-45 and HeLa (Fig. 12c,d) were done in two time points, 48 and 72h, while that in normal cells, WI-38 and NKE, Fig. 12a, b) were done in 48h.

Ability of eriodictyol to block proliferation was studied in 3 mouse tumor cell lines – 4T1, CT-26 and RenCa, both dose- and time- dependently (*Fig. 13*). As seen from the data,eriodictyol blocked proliferation of both 4T1 (*Fig. 13a*) and CT-26 (*Fig. 13b*) dose- and time-dependently with significantly higher efficacy than on RenCa cells (*Fig. 13c*). This is also evident from their IC_{50} values, which clearly show that eriodictyol is much more effective against 4T1 and CT-26 cells than RenCa cell lines. This data not only shows the cytotoxic ability of eriodictyol in a variety of cells, but also helps us in selecting mouse tumor cells for assessing the in vivo anti-tumor activity of eriodictyol in the future.

Figure 13

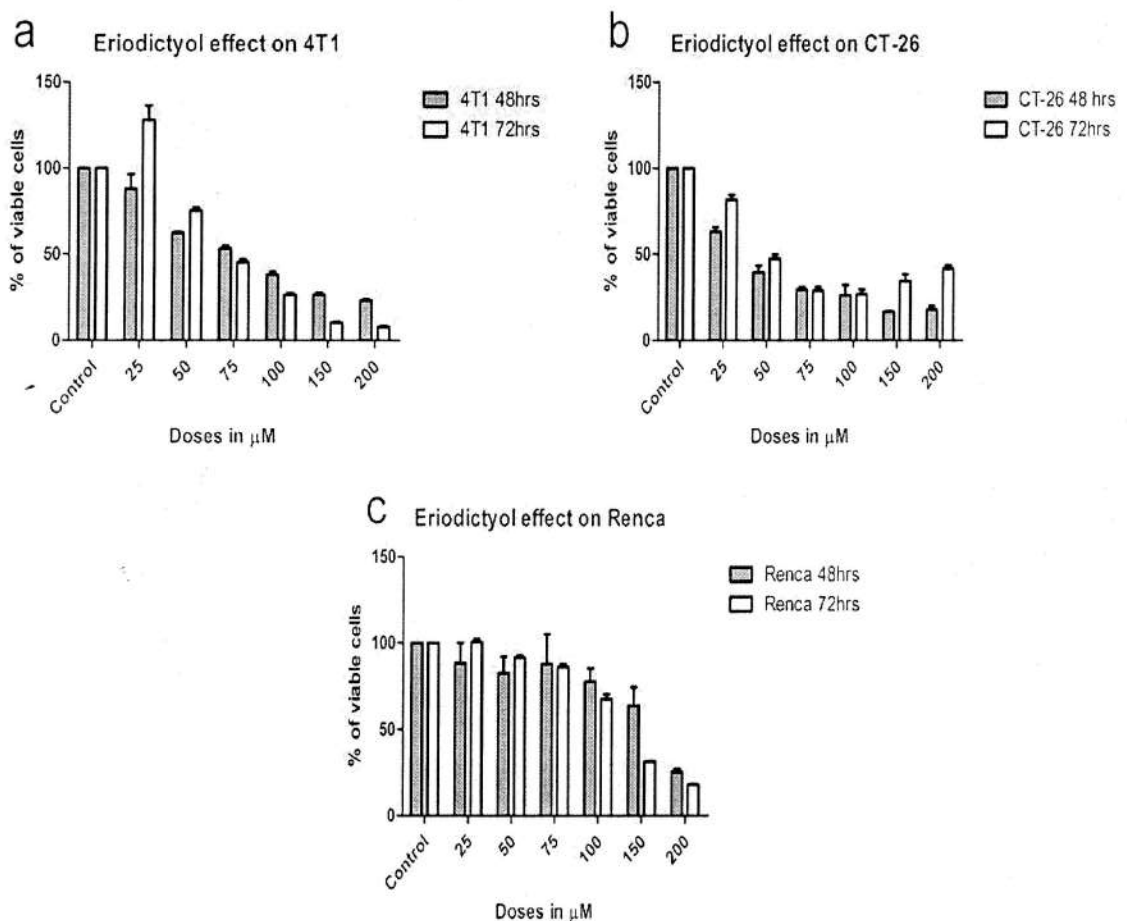


Fig. 13. Eriodictyol blocks proliferation in murine cancer cells. The ability of eriodictyol to block proliferation of mouse cancer cell lines, 4T1 (a), CT-26 (b) and RenCa (c) were determined by MTT assay. Anti-proliferative activity of eriodictyol against mouse cell lines were determined in 48 and 72h.

Eriodictyol induces dose-dependent apoptosis in both human and mouse tumor cells: Since, eriodictyol significantly reduced viability of tumor cells HeLa and SK-RC-45, we wanted to see whether, the reduction in cell viability is due to the ability of eriodictyol to induce apoptosis in tumor cells. In order to address this, 1×10^5 cells were seeded in 6 well plate format for 24 hrs in 2ml of complete RPMI-1640 medium. After 24 hrs, cells were treated for 48 hrs with 50, 100, 125, 150 μM dose of eriodictyol, following which cells were trypsinized and centrifuged at 1200

Figure 14

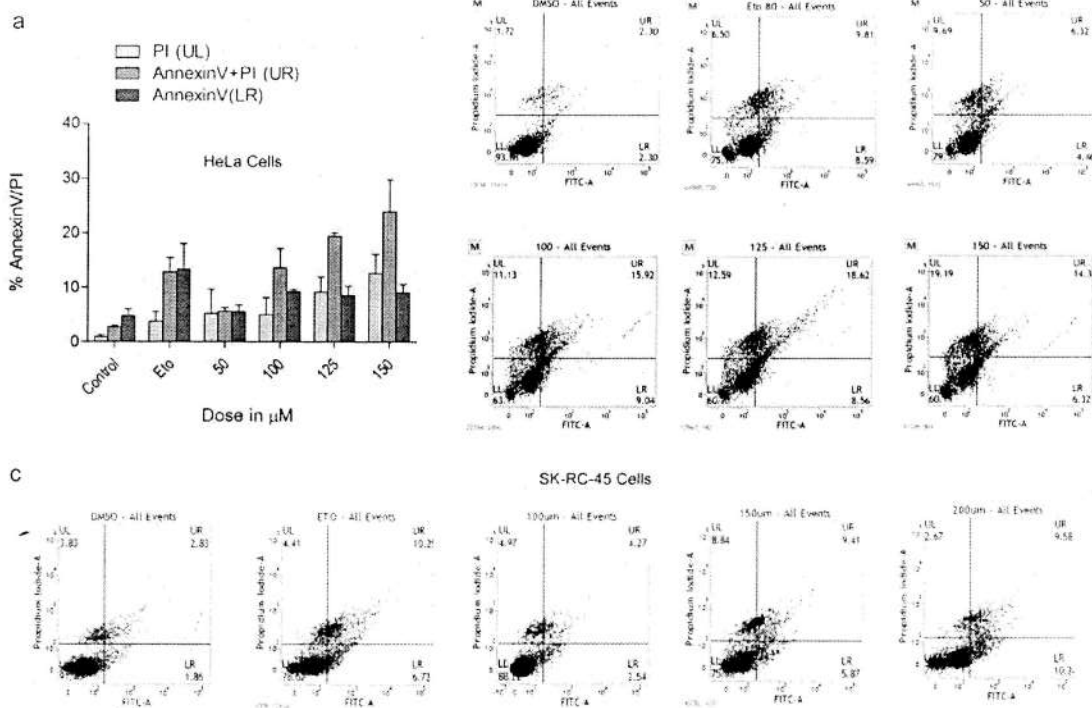


Fig. 14. Eriodictyol induces dose-dependent apoptosis in HeLa cells and SK-RC-45 cells. Ability of eriodictyol in inducing apoptosis in HeLa and SK-RC-45 cells was evaluated by annexin-V/PI staining using flow cytometry. Briefly, cells treated with varying doses of eriodictyol were stained with annexin-V/PI following flow cytometric analysis of the % annexin-V/PI +ve cells, which is indicative of the % cells undergoing apoptosis. At least 10,000 events were acquired using a BD FACSVerser flow cytometer, and data was analyzed using BD FACSuite software. Data shows significant dose-dependent induction of apoptosis in response to eriodictyol as evident from the % cells in UL/UR/LR quadrants which is represented in Fig. 14b and 14c. Fig. 14a shows the mean of 3 independent experiments in HeLa cells.)

rpm for 2 mins. The supernatant was discarded and washed with 1X PBS. 100 μ l of 1X annexin-V binding buffer was added and pellets were resuspended in the binding buffer. 2 μ l of annexin V (stock conc = 50 μ g/250 μ l) was added to the dissolved pellet and incubated for 15 mins at room temperature. Apoptosis induction in cells was determined from the % annexin-V +ve / propidium iodide (PI) +ve cells using BD FACSuite software.

Results shown in Fig. 14 indicate dose-dependent induction of apoptosis in HeLa cells by eriodictyol at 48 hrs as evident from the percentage of annexin-V +ve / PI +ve cell populations

Figure 15

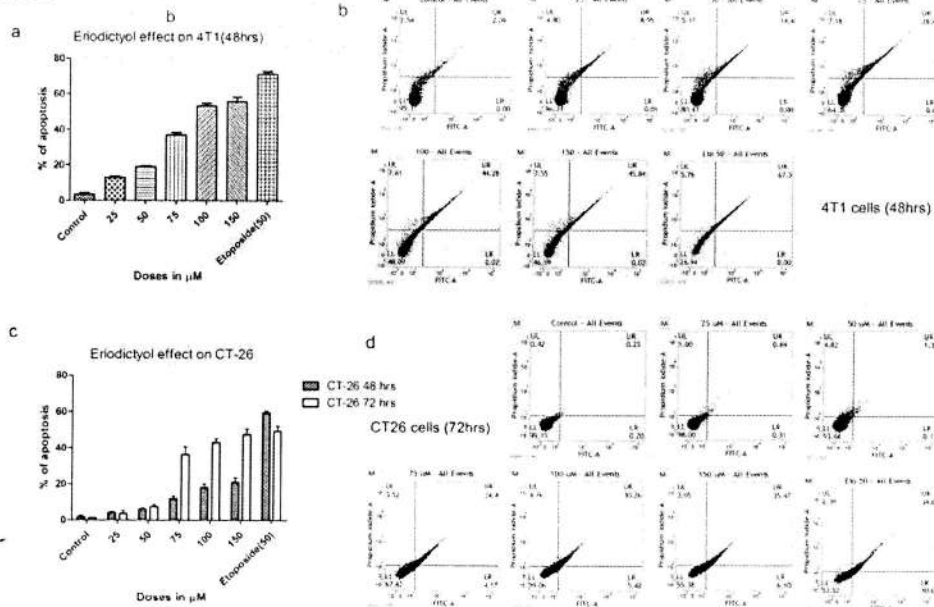


Fig. 15. Eriodictyol induces dose-dependent apoptosis in murine cancer cells. Ability of eriodictyol in inducing apoptosis in mouse cancer cell lines, 4T1 and CT-26 were evaluated by annexin-V/PI staining using flow cytometry. Briefly, cells treated with varying doses of eriodictyol were stained with annexin-V/PI following flow cytometric analysis of the % annexin-V/PI +ve cells, which is indicative of the % cells undergoing apoptosis. At least 10,000 events were acquired using a BD FACSVerser flow cytometer, and data was analyzed using BD FACSuite software. Data show significant dose-dependent induction of apoptosis in response to eriodictyol as evident from the % cells in UL/UR/LR quadrants which is represented in Fig. 15b and 15d. Fig. 15a& 15c show the mean of 3 independent experiments in HeLa cells.)

shown either by the representative density plot (Fig. 14b) or from the bar graph (Fig. 14a). Fig. 14c shows dose-dependent induction of apoptosis in SK-RC-45 cells by eriodictyol, as evidenced by the increasing percentage of cells staining positive for annexin-V/PI. Similar dose-dependent induction of apoptosis in response to eriodictyol was obtained in mouse tumor cells, 4T1 (Fig. 15a&15b) and CT-26 (Fig. 15c & 15d), which show dose-dependent increase in the percentage of cells staining positive for annexinV/7AAD. Although, eriodictyol induces 4T1 apoptosis at 48 hrs at concentrations as low as 25 μ M, its effect on CT-26 at same time point is less pronounced, however, it shows potent ability to induce CT-26 apoptosis at 72 hrs. Fig. 15b and 15d represents annexinV/7AAD density plot of 4T1 and CT-26 cells respectively following treatment with eriodictyol.

Eriodictyol cause SK-RC-45 cells to be arrested at the G2/M-phase of the cell cycle :To further investigate the mechanism of inhibition of cellular proliferation by eriodictyol, its effect on the relative distribution of cells in various phases of cell cycle was determined by propidium iodide staining. Data shows dose-dependent increase in the distribution of cells at the G2/M-phase of the cell cycle, as seen from the histogram (Fig. 16a). Interestingly, increase in the proportion of cells in G2/M-phase was accompanied by decrease in cell population of G1- and S-phase, as seen from Fig. 16b. Since, the critical regulatory step in activating cdc 2 (CDK 1) during progression into mitosis is dephosphorylation of cdc 2 at Thr14 and Tyr15, cdc 2 and p-cdc 2 levels were determined by western blot (Fig. 16c). Data shows time-dependent increase in phosphorylation of cdc 2 at Tyr15 in response to eriodictyol treatment, indicating de-activation of cdc 2 and delaying progression into the mitosis stage, and holding the cells at the G2/M checkpoint. Cdc 2 expression is also decreased time-dependently. A group of phosphatases, namely cdc25 dephosphorylate cdc 2 at Thr14 and Tyr15, thereby activating them. Eriodictyol caused a time-dependent decrease in the expression of cdc 25c but not cdc 25a, thereby blocking dephosphorylation of cdc 2 and hence inhibiting activation. Eriodictyol also caused increase in cyclin B1 expression with time.

Figure 16

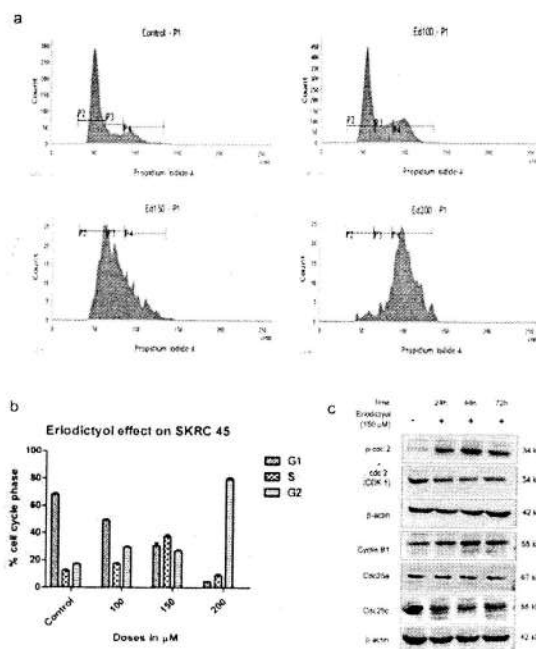


Fig. 16. Eriodictyol induces arrest of SK-RC-45 cells at the G2/M-phase of the cell cycle. Ability of eriodictyol in inducing cell cycle arrest was evaluated by PI staining. For this experiment, double thymidine blocked synchronized human cancer cell, SK-RC-45 was treated with increasing concentrations (100 μM , 150 μM , 200 μM) of Eriodictyol for 24hrs. Post treatment, cells were harvested into single cell suspension and fixed by incubating the cells overnight at -20°C with 75% ethanol. Cells were centrifuged and resuspended in 1XPBS for 2hrs followed by RNaseA (20 μM) treatment for 2hrs at 37°C. Finally, PI was added and incubated for 20 minutes at room temperature. Flow cytometric analysis was immediately performed using a FACS Verse (BD). Data show significant dose-dependent distribution of cells at the G2/M-phase (a-b) in response to eriodictyol. Fig. 16c shows time-dependent expression of key cell cycle regulatory proteins in SK-RC-45 cells treated with 150 μM eriodictyol.

Eriodictyol induces apoptosis by causing disbalance between several pro- and anti-apoptotic proteins: We looked at the molecular events underlying eriodictyol mediated apoptosis in SK-RC-45 and HeLa cells. Western blot data show significant time-dependent increase in expression of the pro-apoptotic DISC components, TNFR1, FADD and TRADD in both SK-RC-45 (*Fig.*

Figure 17 SK-RC-45 Cells

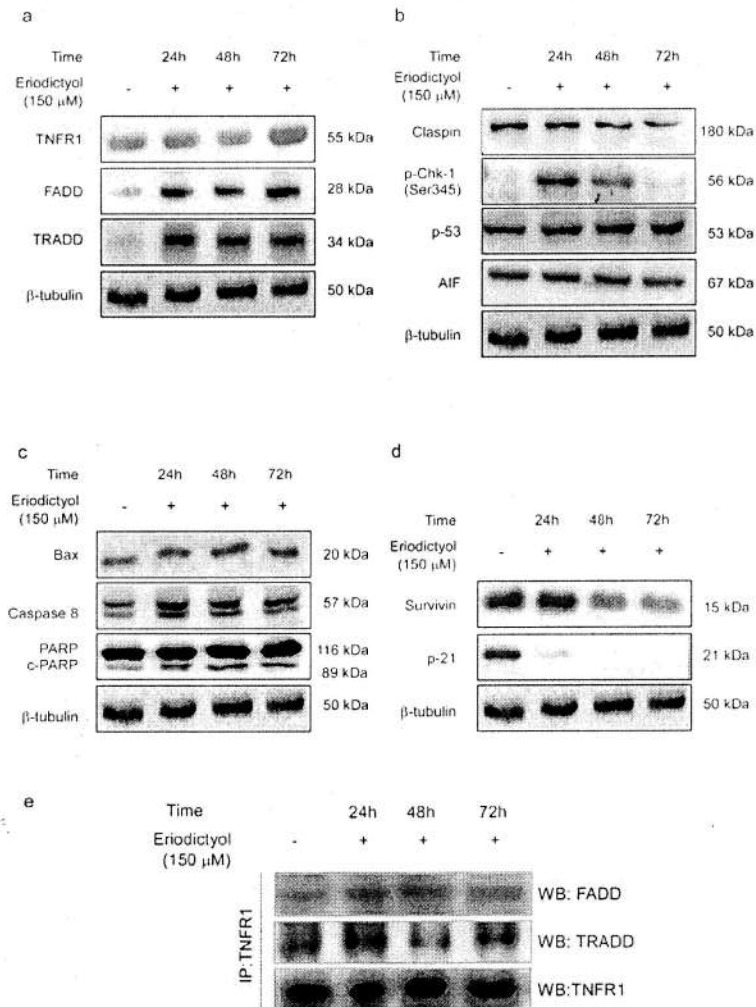


Fig. 17. Eriodictyol induces apoptosis by destabilizing pro- and anti-apoptotic components. a. Induction of receptor components of TNF-dependent apoptotic signaling in response to eriodictyol treatment with time in SK-RC-45 cells. b. Eriodictyol mediated activation of DNA-damage response with time was determined by expression of key proteins associated with DNA-damage. c. Signaling events leading towards activation of caspase-8 and PARP- cleavage in response to time-dependent eriodictyol treatment. d. Expression levels of anti-apoptotic proteins, which assist in cell survival in SK-RC-45 cells treated with eriodictyol for different time points. E. Confirmation of formation of the death inducing signaling complex (DISC) by co-IP with TNF-R1 Ab, and blotting with either TRADD or FADD in response to time-dependent eriodictyol treatment in SK-RC-45 cells.

17a) and HeLa cells (*Fig. 18a*), suggesting formation of the DISC complex. This was confirmed by Co-IP experiments in SK-RC-45 cells, which show both FADD and TRADD to

immunoprecipitate with TNFR1 time-dependently in response to eriodictyol treatment (Fig. 17e). Bax/Bcl2 ratio was found to be altered in both SK-RC-45 (Fig. 17c) and HeLa (Fig. 18a) with consequent activation of caspase-8 and PARP activation, as indicated by increase in their corresponding cleaved products in response to eriodictyol with time. Eriodictyol caused time-

Figure 18 HeLa cells

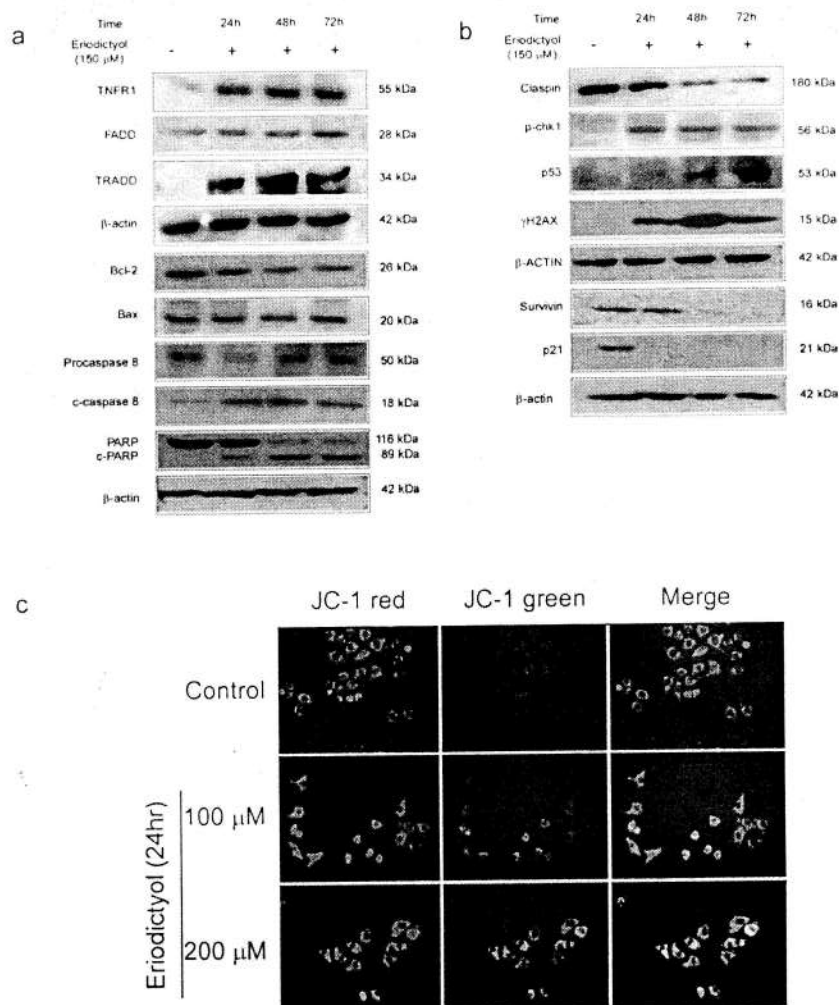


Fig. 18. Eriodictyol induces apoptosis by destabilizing pro- and anti-apoptotic components. a. Induction of receptor components of TNF-dependent apoptotic signaling and events leading towards activation of caspase-8 and PARP- cleavage in response to time-dependent eriodictyol treatment in HeLa cells. **b.** Eriodictyol mediated activation of DNA-damage response with time was determined by expression of key proteins associated with DNA-damage alongwith expression levels of anti-apoptotic proteins, which assist in cell survival in HeLa cells treated with eriodictyol for different time points. **c.** Dose-dependent transition of mitochondrial permeability in HeLa cells by eriodictyol using JC1 staining protocol by visualizing a decrease in JC1 (red) and increase in JC1 (green) signal in response to eriodictyol treatment in HeLa cells.

dependent decrease in the levels of key anti-apoptotic proteins, Survivin and p-21 in both SK-RC-45 (Fig. 17d) and HeLa (Fig. 18b) cells, thereby confirming that eriodictyol not only cause

upregulation in pro-apoptotic proteomes, but a significant decrease in survival proteins thereby leading towards a pro-apoptotic outcome. In parallel, eriodictyol also caused time-dependent modulation in several proteins characteristic of DNA damage, like Chk-1, p-Chk-1, γ -H2AX and claspin in both SK-RC-45 (Fig. 17b) and HeLa (Fig. 18b) cells. This is indicative of a possible DNA damaging role of eriodictyol in cancer cells, which might eventually lead to induction of apoptotic signaling events.

Figure 19

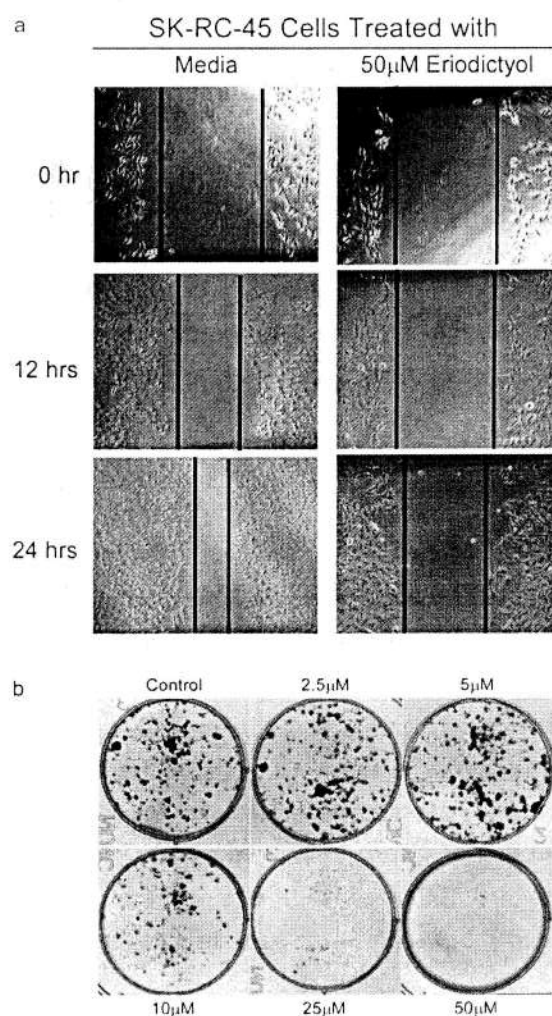


Fig. 19. Eriodictyol inhibits cell migration and clonogenicity of tumor cells at concentrations much lower than that required to induce apoptosis. a. Wound healing assay was performed in SK-RC-45 cells to check the effect of eriodictyol on migration. Uniform scratches were applied to a monolayer of SK-RC-45 cells either treated or not with 50µM eriodictyol in serum free media. Migration of the cells were initiated by adding serum containing medium, and closure of gap was monitored for different time intervals and photographed. **b.** For clonogenicity assay, cells either non-treated or treated with varying doses of eriodictyol, were plated at very low density (200 cells/well in 6well plate), grown for either 8/10 days, fixed with 3.7% formaldehyde, stained with 0.05% crystal violet and image was captured using Gel Doc XR+ (Bio-Rad).

Assessing the ability of eriodictyol in blocking migration and clonogenicity in SK-RC-45 : Migration of tumor cells is one of the significant properties on which metastatic ability of tumor cells depend. Hence, we wanted to check whether, eriodictyol can also cause reduction in migration of tumor cells at least *in vitro*, and at concentrations much below that is required to induce apoptosis. 25×10^3 cells were placed in each well of 6 well plates for 24hrs in CO₂ incubator. After 24hrs the media was replaced with fresh complete RPMI-1640 and treated with the compound for 48 hrs. After 48hrs the complete media was discarded and serum free media was added. Uniform scratches were given in each well. Fresh serum free media was added. At an interval of 0, 12, 24 hrs cells were observed for the cell migration under microscope. The rate at which the gap created by the scratch fills gives an index of cellular migration. Results show that while the gap in the non-treated SK-RC-45 cells fills much faster indicative of faster migration, in the treated cells, there is significant reduction in the migration of tumor cells, as shown in the photomicrograph in *Fig. 19a*.

For clonogenicity assay, cells were plated at very low density (200 cells/well in 6 well plate), grown for either 8/10 days, fixed with 3.7% formaldehyde, stained with 0.05% crystal violet and image was captured using Gel Doc XR+ (Bio-Rad). Eriodictyol significantly inhibits colony forming ability of the SK-RC-45 tumor cells at concentrations as low as 10 μ M (*Fig. 19b*) with an almost complete abrogation of colony forming ability of the cells at 25 μ M dose of eriodictyol (*Fig. 19b*).

Objective 3. To determine the efficacy of 2-3 lead compounds in preventing chronic inflammation induced pathogenesis in animal models

Mouse paw edema anti-inflammatory assay for kaempferol: Anti-inflammatory efficacy of kaempferol was also studied in mouse paw edema model. The animal experiment was carried out with approval from Institutional Animal Ethical Committee of Defense Research Laboratory, Tezpur. Thirty Swiss Albino mice were divided into five groups. Group I was maintained as negative control. Group II was intraperitoneally (i.p.) injected with dimethyl sulphoxide (DMSO). The third group (Group III) was treated i.p. with indomethacin, a standard non-steroidal anti-inflammatory drug (10 mg/kg). The last two groups (Group IV and Group V) were injected with 1/10 (35 mg/kg) and 1/20 (17.5 mg/kg) of LD-50_{mouse} dose (350 mg/kg) of kaempferol, respectively using i.p. route. After 3 hours of treatment in Group II-V, acute inflammation was promoted by the sub-cutaneous injection of 1% carrageenan solution in the sub-plantar space of the right hind paw, while left paws were injected with 50 μ l normal saline. Time-dependent reduction in paw volume was measured at 0, 2 and 24 hours as compared to control using a plethysmometer. Paw volume was significantly reduced in the kaempferol treated samples as compared to the carrageenan-induced samples (Figure 20A). Paw tissues were harvested for mRNA and protein expression using RT-PCR and western blot analysis, respectively. Both gene and protein expression of COX-2, an important marker in carrageenan-induced inflammation was modulated in the kaempferol treated groups. In addition, activation of the transcription factors STAT3 and NF-kB were also reduced in the kaempferol-treated groups (Figure 20B, C). Hence, kaempferol reduces the expression of

COX-2, an important marker in carrageenan-induced mouse paw edema, as well as the activation of the important transcription factors for COX-2 regulation, STAT3 and NF- κ B.

Figure 20

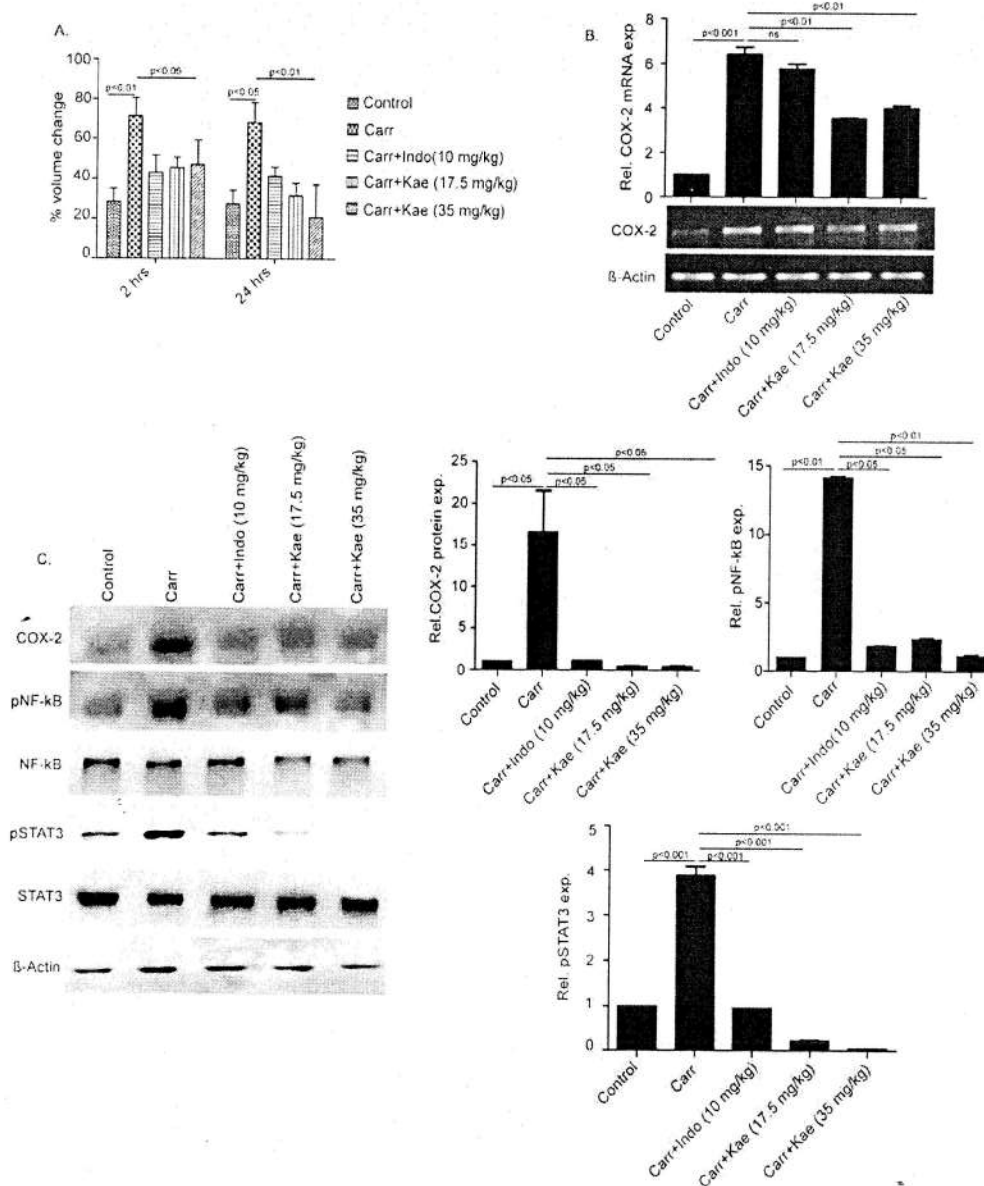


Figure 20: Kaempferol reduces carrageenan-induced paw edema volume, COX-2 expression and activation of NF- κ B and STAT3. The mean percent change in paw volume of different groups of mice was measured using a plethysmometer at 2 and 24 hours (A). Harvested paw tissues were analyzed for mRNA expression of COX-2 using semi-quantitative RT-PCR(B). The paw lysates were analyzed for expression of COX-2 and phospho and non-phosphorylated forms of STAT3 and NF- κ B (C). The quantitative result of western blots is also presented.

In addition, histochemical studies of the mice paws were done using hematoxylin and eosin staining to check for neutrophil infiltration levels in the control and treated paws (Figure 21 A-E). Paws were collected after induction of edema and fixed in 10% formalin. Whole paws without skin were decalcified with 10% EDTA (pH 7.4) at 4°C for 3 weeks. EDTA was replaced weekly. The decalcification process and the end point were assessed with a surgical blade. Then the paws were dehydrated, cleared and embedded in paraffin and stained with H&E stain. Increased neutrophil infiltration was found in the carrageenan treated paw (Fig 21B) as compared to the control paw injected with normal saline (Fig 21A), while reduced infiltration was observed in indomethacine and kaempferol treated paws (Fig 21C, D, E). These experiments together proves the anti-inflammatory efficacy of kaempferol in carrageenan-induced mouse paw edema.

Figure 21

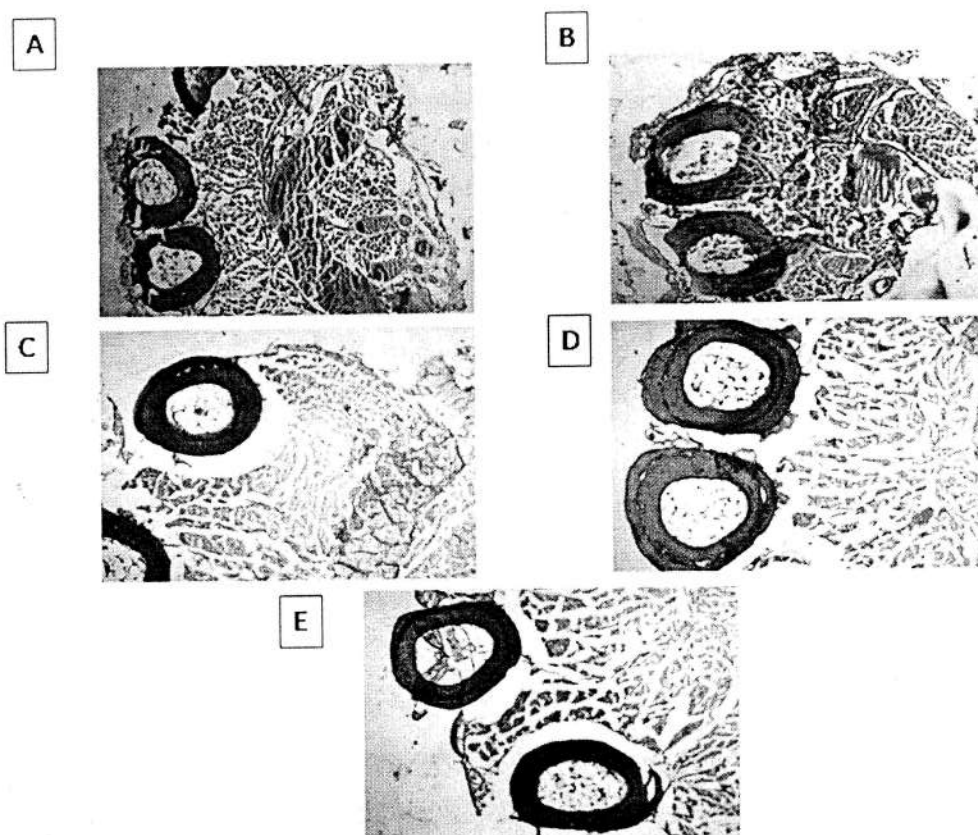


Figure 21: Hematoxylin and Eosin staining of saline and carrageenan injected paws: (A) Left paw injected with normal saline, (B) Right paw injected with carrageenan, (C) Intraperitoneally injected with Indomethacine (10 mg/kg) while right paw injected with carrageenan, (D & E) Intraperitoneally injected with kaempferol (17.5 mg/kg and 35 mg/kg respectively) while right paw injected with carrageenan.

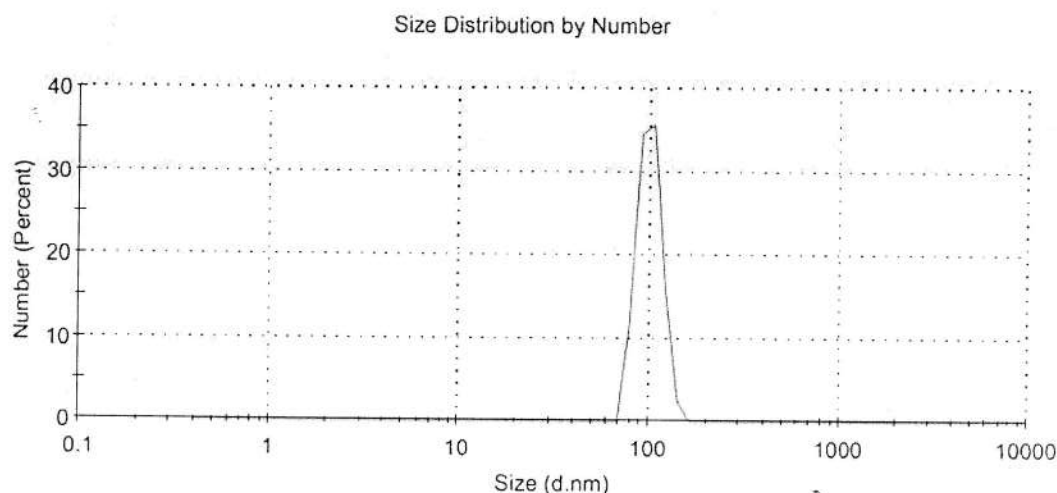
The above findings clearly bolsters the ability of kaempferol to attenuate the expression of COX-2, an important pro-inflammatory mediator, by modulating the activation of the two transcription factors, STAT3 and NF- κ B, irrespective of the inducer of inflammation (in our case, IL-6 and carrageenan).

Objective 4. To generate derivatives of parent compounds by functional group modifications to enhance their anti-cancer and/or anti-atherosclerotic activity

Since significant amounts (in grams) of the three polyphenols studied e.g. kaempferol, biochanin A and eriodictyol would be required for any modification of functional groups by organic synthetic procedures, while the amounts of the polyphenols commercially received were in very small amounts (in milligrams), we decided to study the objective 4 in an alternative way. Two polyphenols (kaempferol and biochanin A) were used to synthesize chitosan-based nanoparticles for studying their efficacy. Chitosan (Cs) [1.75mg/ml] was dissolved in 1% acetic acid by stirring at room temp. for 2 hrs. 100 μ l of the Kae/BCA solution (8.5 μ l in 91.5 μ l DMSO) was added to 1 ml of the stirred Cs solution. 1 ml of 0.4 mg/ml TPP aq. solution was added dropwise to the Cs solution under stirring. In each drop only 80 μ l of TPP solution was added and waited for 2 minutes before addition of another drop. After completion of addition, stirring for another half an hour was allowed. The solution was centrifuged at a speed of 10,000 rpm at 4°C for 1 hour. The residue was re-dispersed in molecular biology grade water and washing was repeated twice for 1 hour. Finally it was resuspended in 1 mL molecular biology grade water. For physical assessment of nanoparticles, DLS (Dynamic Light Scattering) was performed. DLS data for both the compounds (BCA and Kae) (Figures 21 and 22) shows the successful formation of nanoparticles at 100 nm size for both.

Figure 21

A.



B.

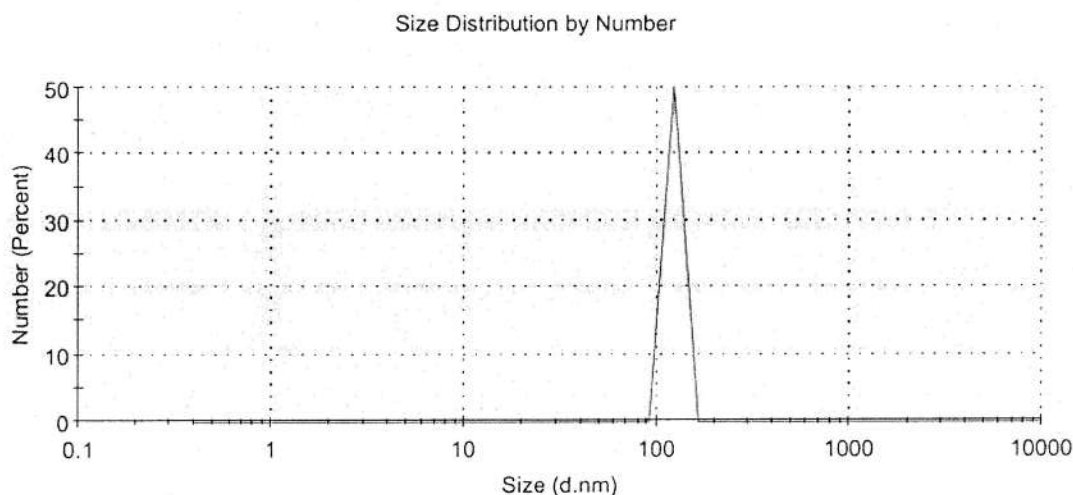


Figure 21: DLS data of chitosan-based nanoparticles using (A) BCA and Kaempferol (B)

Further characterization of the nanoparticles synthesized in this process is undergoing in the laboratory. Efficacy of these nanoparticles in cell culture model will be tested to study if these are more effective than normal polyphenols.

B2. Summary and Conclusions of the Progress made so far: The current project aims towards identifying polyphenol compounds which by virtue of their anti-inflammatory properties, will be effective against chronic inflammation induced disease pathogenesis, like cancer, atherosclerosis and understanding their mechanism of action. Hence screening of potential compounds with anti-inflammatory efficacy was performed as a part of Objective 1. From a pool of 17 polyphenols, three potent compounds e.g. kaempferol, biochanin A and eriodictyol have been selected to study their mechanism of action against inflammation or cancer. All three compounds showed potent anti-inflammatory activity in blocking LPS- and/or IL-6-induced expression of several pro-inflammatory genes in the human monocytic cell line THP-1. In the present study, kaempferol and biochanin A have been studied for its mechanism of anti-inflammatory activity (**work mostly carried out in Tezpur University**) and eriodictyol for its possible anti-cancer efficacy, more specifically against uncontrolled cell proliferation and metastasis (**work mostly carried out in Bose Institute**). Kaempferol, inhibited expression of inflammatory mediator COX-2 in IL-6-induced THP-1 macrophage-like cell lines via inhibition of NF-kB and STAT3 activation. The compound also inhibited the nuclear translocation of transcription factor suggesting their efficacy against transcription of pro-inflammatory genes. For the first time mechanism of COX-2 inhibition by kaempferol in IL-6 induced cells has been described.

We have studied the anti-inflammatory activity of biochanin A (BCA) in the same cell culture model. The molecular targets of BCA are distinct from kaempferol as it inhibited STAT3 activation in a dose-dependent manner; and showed minimal inhibition of NF-kB activity at lower concentrations. This suggests BCA's preferential efficacy against STAT3 in comparison to NF-kB. Since, BCA showed significant inhibition of IL-6-induced expression of MCP-1, pro-inflammatory mediator responsible for macrophage migration and adhesion [25], we studied effect of BCA on migration and adhesion. Our data suggested BCA induced remarkable inhibition of migration and adhesion of macrophages.

Anti-proliferative activity of eriodictyol was assessed by MTT assay in at least two different tumor cell lines, SK-RC-45 and HeLa and two normal cell lines WI38 and NKE. Significant inhibition of cellular proliferation was observed in the tumor cells compared to normal cell lines which showed negligible effect. To find out whether the observed anti-proliferative effect of eriodictyol was due to its ability to induce apoptosis, annexin-V/PI staining followed by FACS analysis was performed in both HeLa and SK-RC-45. Eriodictyol showed significant dose-dependent apoptosis in both HeLa cells as well as in SK-RC-45 cells. To test the efficacy of eriodictyol in suppressing metastatic ability of the cells, wound healing assay was performed with SK-RC-45 cells at concentration insufficient in inducing apoptosis. Result shows that 50 μ M eriodictyol suppressed the migration of SK-RC-45 cells. These *in vitro* studies showed potential of eriodictyol as an anti-cancer compound which may be therapeutically used for treating chronic inflammation induced carcinogenesis.

Data from animal experiments suggested kaempferol-mediated inhibition of mouse paw edema confirming its anti-inflammatory activity. Detailed study revealed that activation of COX-2 by carrageenan has been reduced by kaempferol via inhibition of STAT3 and NF-kB. This study suggested STAT3 and NF-kB are common targets of kaempferol-mediated attenuation of COX-2 expression irrespective of inflammatory stimulus. Chitosan-based nanoparticles of kaempferol and biochanin A has also been synthesized to study their effect on inflammation using cell culture models.

B3. Details of New Leads Obtained, if any:

- Our study suggested Biochanin A (BCA) inhibits the activation of STAT3 while augmenting p38 MAPK activation in a specific condition. From existing reports and preliminary experiments in our laboratory, we speculate that the inhibitory activity of BCA on STAT3 is dependent upon p38 MAPK which has four different isoforms, namely, alpha, beta, gamma, delta p38 MAPK. These 4 isoforms are differentially expressed in different cells and conditions [26]. Hence, our future study would be directed to know which isoform(s) of p38MAPK is/are playing important role in BCA-mediated inhibition of STAT3.

- STAT3 and NF-kB are reported to interact physically in conditions e.g. cancer cells [27]. Our study on inhibition of IL-6 induced COX-2 by kaempferol suggested involvement of STAT3 and NF-kB. Our next experiment would be directed to unravel whether kaempferol disrupts the liaison between these two transcription factors in our inflammation model.
- Our study suggested eriodictyol to be a potent anti-cancer agent using various cancer cell lines. Based on the data our next experiment are ongoing to prove its efficacy in metastasis models using 4T1 cell injected Balb/C mice.
- Our study suggested anti-inflammatory efficacy of kaempferol and biochanin A in cell culture and acute animal models. An animal model of chronic inflammation (e.g. psoriasis) would be studied to understand the effect of these polyphenols.

B4. Details of Publications & Patents, if any: See Annexure I

Annexure I

Publications from the project:

- **Basu, Anandita**, Anindhya Sundar Das, Manoj Sharma, Manash Pratim Pathak, Pronobesh Chattopadhyay, Kaushik Biswas, and Rupak Mukhopadhyay (2017): "STAT3 and NF- κ B are common targets for kaempferol-mediated attenuation of COX-2 expression in IL-6-induced macrophages and carrageenan-induced mouse paw edema." *Biochemistry and Biophysics Reports* 12, 54-61. (Elsevier) (PDF attached)
- **Basu, Anandita**, Anindhya S. Das, Munmi Majumder, and Rupak Mukhopadhyay (2016): "Antiatherogenic roles of dietary flavonoids chrysin, quercetin, and luteolin." *Journal of Cardiovascular Pharmacology* 68(1) 89-96. (Wolters Kluwer) (PDF attached).
- **Shibjyoti Debnath**, Pravat Parida, Barun Mahata, Anandita Basu, Rupak Mukhopadhyay and Kaushik Biswas. "The plant derived flavonoid eriodictyol drives G2/M arrest and induces apoptosis to inhibit cancer cell proliferation and metastasis." (Manuscript under preparation).
- **Anandita Basu**, Anindhya Sundar Das, Shibjyoti Debnath, Kaushik Biswas and Rupak Mukhopadhyay. "Biochanin A inhibits STAT3 activation in IL-6-induced macrophages through augmentation of p38 MAPK expression". (Manuscript under preparation).
- **Workshops and seminars attended:**
 - Workshop on 'Advanced Techniques in Cell and Molecular Biology' held at IIT Guwahati, organised by Department of Biotechnology, Indian Institute of Technology Guwahati (24-26 June, 2014).
 - Poster presented: '**Plant-based polyphenols and their effect against atherogenesis**' at National Seminar on 'Recent advances in Biotechnology Research in North-East India: Challenges and Prospects,' held at Department of Molecular Biology and Biotechnology, Tezpur University (Nov 27-29, 2014).
 - Poster presented: "**Anti-inflammatory Efficacy of Kaempferol on COX-2 Gene Expression in Human THP1 Cells**" at International conference on 'Molecular Signaling: Recent Trends in Biosciences', organised by Department of Zoology, North-Eastern Hill University, Shillong, Meghalaya, India (Nov 20-22, 2015).
 - Poster presented: "**Kaempferol attenuates COX-2 expression in IL-6-induced macrophages and carrageenan-induced mouse paw edema by targeting STAT3 and NF- κ B**" at *NextGen Genomics, Biology, Bioinformatics and Technologies (NGBT) Conference, organized by SciGenom Research Foundation (SGRF), Chennai, India 2017.*

Annexure II

Visits to collaborating laboratories as a part of this project study

1. Visit of Dr. K. Biswas, PI from Bose Institute to Tezpur University laboratory (Nov 2014)

Purpose of the visit: To train the JRF on PBMC isolation and treatment with anti-inflammatory agent

It is important to establish in vitro model with primary cell where anti-inflammatory compounds can be studied for mechanism. The student working on this project in TU laboratory was trained with isolation of peripheral blood monocyctic cells (PBMCs) for this purpose.

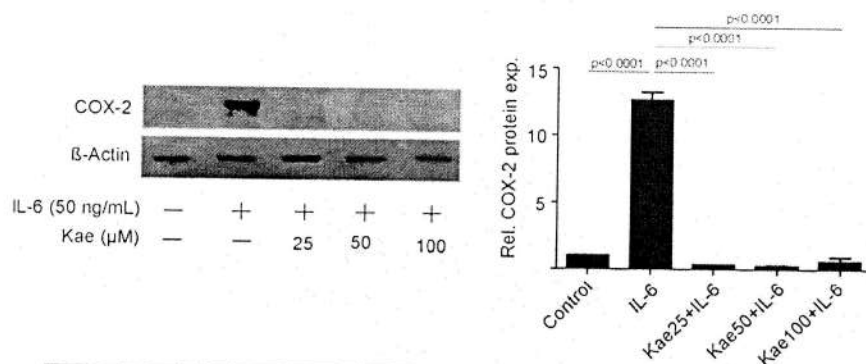
Methodology:

Blood was collected from healthy individuals with due permission from the Institute Ethical Committee, Tezpur University. 3 mL of Histopaque-1077 (Sigma-Aldrich, USA) was added to a 15-mL conical centrifuge tube and brought to room temperature. 3 mL of whole blood was carefully layered onto the Histopaque-1077 followed by centrifugation at 400g for 30 minutes at room temperature. After centrifugation, the upper layer was carefully aspirated with a Pasteur pipette to within 0.5 cm of the opaque interface containing mononuclear cells, while the upper layer was discarded. The opaque interface was carefully transferred to a clean conical centrifuge tube. The cells were washed with 10 mL of 1X phosphate buffered saline (PBS) solution and gently mixed, followed by centrifugation at 250g for 10 minutes. The supernatant was discarded, while the pellet was resuspended with 5 mL of PBS and washing was repeated. The cell pellet was finally resuspended cell in 0.5 mL of RPMI medium. Erythrocytes and granulocytes pelleted to the bottom of the centrifuge tube while mononuclear cells formed a band at the interface between the Histopaque-1077 and the plasma.

Kaempferol treatment in PBMC's:

2-3 X 10⁶ of the isolated PBMC's were added in each well and incubated for 2 hours at 37°C and 5% CO₂ in the CO₂ incubator. The cells were then pre-treated with kaempferol at three different concentrations for 6 hours followed by IL-6 (50 ng/mL) for 2 hours. Thereafter, the cells were harvested using RIPA buffer (containing protease inhibitor) for western blot analysis.

Result: Western blot analysis of COX-2 expression was checked using beta actin as the endogenous control. Increased COX-2 expression was seen in IL-6-induced cells and its expression was markedly reduced in the kaempferol-treated samples (Figure 1)



Kaempferol inhibits the expression of COX-2 in IL-6 induced PBMC's

2. Visit of Dr. Rupak Mukhopadhyay, PI from Tezpur University to the Bose Institute (May 2016)

Purpose of visit: Scientific discussion and writing draft of manuscript.

3. Visit of Research fellow working in TU laboratory to the laboratory of Dr. K. Biswas, Bose Institute Kolkata (July-Aug 2017).

Purpose of visit: Ms. Anandita Basu working in the project in TU visited Bose Institute for synthesis of chitosan-based nanoparticles with kaempferol and biochanin A

References:

1. Liang, Yu-Chih, Ying-Tang Huang, Shu-Huei Tsai, Shoen-Yn Lin-Shiau, Chieh-Fu Chen, and Jen-Kun Lin. "Suppression of inducible cyclooxygenase and inducible nitric oxide synthase by apigenin and related flavonoids in mouse macrophages." *Carcinogenesis* 20, no. 10 (1999): 1945-1952.
2. Park, S. E., K. Sapkota, S. Kim, H. Kim, and S. J. Kim. "Kaempferol acts through mitogen-activated protein kinases and protein kinase B/AKT to elicit protection in a model of neuroinflammation in BV2 microglial cells." *British journal of pharmacology* 164, no. 3 (2011): 1008-1025.
3. García-Mediavilla, Victoria, Irene Crespo, Pilar S. Collado, Alejandro Esteller, Sonia Sánchez-Campos, María J. Tuñón, and Javier González-Gallego. "The anti-inflammatory flavones quercetin and kaempferol cause inhibition of inducible nitric oxide synthase, cyclooxygenase-2 and reactive C-protein, and down-regulation of the nuclear factor kappaB pathway in Chang Liver cells." *European journal of pharmacology* 557, no. 2-3 (2007): 221-229.
4. O'Leary, Karen A., Sonia de Pascual-Tereasa, Paul W. Needs, Yong-Ping Bao, Nora M. O'Brien, and Gary Williamson. "Effect of flavonoids and vitamin E on cyclooxygenase-2 (COX-2) transcription." *Mutation Research/Fundamental and Molecular Mechanisms of Mutagenesis* 551, no. 1 (2004): 245-254.
5. Kothari, Poonam, Roberto Pestana, Rim Mesraoua, Rim Elchaki, KM Faisal Khan, Andrew J. Dannenberg, and Domenick J. Falcone. "IL-6-mediated induction of matrix metalloproteinase-9 is modulated by JAK-dependent IL-10 expression in macrophages." *The Journal of Immunology* 192, no. 1 (2014): 349-357.
6. Kishimoto, Tadimitsu. "IL-6: from its discovery to clinical applications." *International immunology* 22, no. 5 (2010): 347-352.
7. Scheller, Jürgen, Athena Chalaris, Dirk Schmidt-Arras, and Stefan Rose-John. "The pro- and anti-inflammatory properties of the cytokine interleukin-6." *Biochimica et Biophysica Acta (BBA)-Molecular Cell Research* 1813, no. 5 (2011): 878-888.
8. Lipsky, P. E., and P. C. Isakson. "Outcome of specific COX-2 inhibition in rheumatoid arthritis." *The Journal of rheumatology. Supplement* 49 (1997): 9-14.
9. Kang, R. Y., J. Freire-Moar, E. C. C. Q. Sigal, and C-Q. Chu. "Expression of cyclooxygenase-2 in human and an animal model of rheumatoid arthritis." *Rheumatology* 35, no. 8 (1996): 711-718.
10. Yalcin, Basak, Gaye Guler Tezel, Nilufer Arda, Mustafa Erman, and Nuran Alli. "Vascular endothelial growth factor, vascular endothelial growth factor receptor-3 and cyclooxygenase-2 expression in psoriasis." *Analytical and quantitative cytology and histology* 29, no. 6 (2007): 358-364.

11. Stark, Katarina, Hans Törmä, and Ernst H. Oliw. "Co-localization of COX-2, CYP4F8, and mPGES-1 in epidermis with prominent expression of CYP4F8 mRNA in psoriatic lesions." *Prostaglandins & other lipid mediators* 79, no. 1-2 (2006): 114-125.
12. Raisz, Lawrence G. "Pathogenesis of osteoporosis: concepts, conflicts, and prospects." *The Journal of clinical investigation* 115, no. 12 (2005): 3318-3325.
13. Richards, J. B., L. Joseph, K. Schwartzman, N. Kreiger, A. Tenenhouse, and D. Goltzman. "The effect of cyclooxygenase-2 inhibitors on bone mineral density: results from the Canadian Multicentre Osteoporosis Study." *Osteoporosis international* 17, no. 9 (2006): 1410-1419.
14. Kawano, Takayuki, Josef Anrather, Ping Zhou, Laibaik Park, Gang Wang, Kelly A. Frys, Alexander Kunz, Sunghee Cho, Marcello Orio, and Costantino Iadecola. "Prostaglandin E 2 EP1 receptors: downstream effectors of COX-2 neurotoxicity." *Nature medicine* 12, no. 2 (2006): 225.
15. Tsujii, Masahiko, Sunao Kawano, Shingo Tsuji, Hitoshi Sawaoka, Masatsugu Hori, and Raymond N. DuBois. "Cyclooxygenase regulates angiogenesis induced by colon cancer cells." *cell* 93, no. 5 (1998): 705-716.
16. Simmons, Daniel L., Regina M. Botting, and Timothy Hla. "Cyclooxygenase isozymes: the biology of prostaglandin synthesis and inhibition." *Pharmacological reviews* 56, no. 3 (2004): 387-437.
17. Lesina, Marina, Magdalena U. Kurkowski, Katharina Ludes, Stefan Rose-John, Matthias Treiber, Günter Klöppel, Akihiko Yoshimura et al. "Stat3/Socs3 activation by IL-6 transsignaling promotes progression of pancreatic intraepithelial neoplasia and development of pancreatic cancer." *Cancer cell* 19, no. 4 (2011): 456-469.
18. Gao, Sizhi Paul, Kevin G. Mark, Kenneth Leslie, William Pao, Noriko Motoi, William L. Gerald, William D. Travis et al. "Mutations in the EGFR kinase domain mediate STAT3 activation via IL-6 production in human lung adenocarcinomas." *The Journal of clinical investigation* 117, no. 12 (2007): 3846-3856.
19. Hirano, Toshio, Katsuhiko Ishihara, and Masahiko Hibi. "Roles of STAT3 in mediating the cell growth, differentiation and survival signals relayed through the IL-6 family of cytokine receptors." *Oncogene* 19, no. 21 (2000): 2548.
20. Kim, Jong-Bin, Ah-Reum Han, Eun-Young Park, Ji-Yeon Kim, Woong Cho, Jun Lee, Eun-Kyoung Seo, and Kyung-Tae Lee. "Inhibition of LPS-induced iNOS, COX-2 and cytokines expression by poncirin through the NF- κ B inactivation in RAW 264.7 macrophage cells." *Biological and Pharmaceutical Bulletin* 30, no. 12 (2007): 2345-2351.
21. Park, Young-Mi, Jong-Heon Won, Kyung-Jin Yun, Jong-Hoon Ryu, Yong-Nam Han, Seung-Ki Choi, and Kyung-Tae Lee. "Preventive effect of Ginkgo biloba extract (GBB) on the lipopolysaccharide-induced expressions of inducible nitric oxide synthase and cyclooxygenase-2 via suppression of nuclear factor- κ B in RAW 264.7 cells." *Biological and Pharmaceutical Bulletin* 29, no. 5 (2006): 985-990.

22. Terstegen, Lara, Petros Gatsios, Johannes G. Bode, Fred Schaper, Peter C. Heinrich, and Lutz Graeve. "The inhibition of interleukin-6-dependent STAT activation by mitogen-activated protein kinases depends on tyrosine 759 in the cytoplasmic tail of glycoprotein 130." *Journal of Biological Chemistry* 275, no. 25 (2000): 18810-18817.
23. Ahmed, Simi T., and Lionel B. Ivashkiv. "Inhibition of IL-6 and IL-10 signaling and Stat activation by inflammatory and stress pathways." *The Journal of Immunology* 165, no. 9 (2000): 5227-5237.
24. Decker, Thomas, and Pavel Kovarik. "Serine phosphorylation of STATs." *Oncogene* 19, no. 21 (2000): 2628.
25. Park, Keun Hyung, Tae Hoon Lee, Chan Woo Kim, and Jiyoung Kim. "Enhancement of CCL15 expression and monocyte adhesion to endothelial cells (ECs) after hypoxia/reoxygenation and induction of ICAM-1 expression by CCL15 via the JAK2/STAT3 pathway in ECs." *The Journal of Immunology* 190, no. 12 (2013): 6550-6558.
26. Korb, Adelheid, Makiyeh Tohidast-Akrad, Erdal Cetin, Roland Axmann, Josef Smolen, and Georg Schett. "Differential tissue expression and activation of p38 MAPK α , β , γ , and δ isoforms in rheumatoid arthritis." *Arthritis & Rheumatology* 54, no. 9 (2006): 2745-2756.
27. Grivennikov, Sergei I., and Michael Karin. "Dangerous liaisons: STAT3 and NF- κ B collaboration and crosstalk in cancer." *Cytokine & growth factor reviews* 21, no. 1 (2010): 11-19.

**Statement of Expenditure referred to in para 9 of the Utilization Certificate
(CONSOLIDATED)**

Showing grants received from the Department of Biotechnology and the expenditure incurred during the period from 3rd March 2014 to 2nd September 2017.

(Rs. in lakhs)

Financial Year	03/03/2014- 31/03/2014	01/04/2014- 31/03/2015	01/04/2015- 31/03/2016	01/04/2016- 31/03/2017	01/04/2017- 02/09/2017	Total
Installment	1st		2nd	3rd		
Equipments	15.00	0.00	0.00	0.00		15.00000
(i) Human resource	2.11	0.00	3.66	3.35		9.12000
(ii) Consumables	8.00	0.00	7.98	6.20		22.18000
(iii) Travel	0.50	0.00	0.21	0.11		0.82000
(iv) Contingency	0.50	0.00	0.20	0.25		0.95000
(v) Overheads	0.75	0.00	0.29	0.11		1.15000
	26.86		12.34	10.02		49.22000

B. Lamin

EXPENDITURE						
Financial Year	03/03/2014-31/03/2014	01/04/2014-31/03/2015	01/04/2015-31/03/2016	01/04/2016-31/03/2017	01/04/2017-02/09/2017	Total
Equipments	0.0	15.32153	0.0	0.0	0.0	15.32153
(i) Human resource	0.0	1.88267	3.54000	3.35300	0.34322	9.11889
(ii) Consumables	0.0	7.97601	7.19923	0.44921	6.42257	22.04702
(iii) Travel	0.0	0.21312	0.10511	0.14744	0.23646	0.70213
(iv) Contingency	0.0	0.44383	0.25591	0.25000	0.0	0.94974
(v) Overheads	0.0	0.64309	0.18125	0.18023	0.14329	1.14786
	0	26.48025	11.2815	4.37988	7.14554	49.28717

CONSOLIDATED 3 YEAR STATEMENT OF EXPENDITURE				
	Fund Received	Interest earned	Expenditure	Balance
Equipments	15.00000		15.32153	(-)0.32153
(i) Human resource	9.12000		9.11889	0.00111
(ii) Consumables	22.18000		22.04702	0.13298
(iii) Travel	0.82000		0.70213	0.11787
(iv) Contingency	0.95000		0.94974	0.00026
(v) Overheads	1.15000		1.14786	0.00214
Interest		0.27507		0.27507
Total	49.22000	0.27507	49.28717	0.20790

Rupak Mukhopadhyay 25/11/18
(PROJECT INVESTIGATOR)

Dr. RUPAK MUKHOPADHYAY
Assistant Professor
Department of M B B T
TEZPUR UNIVERSITY
Napaam, Tezpur, Assam, 784028

B
(HEAD OF THE INSTITUTE)

Registrar
Tezpur University

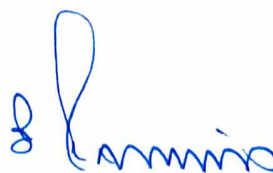
B. G. G. G.
31/11/18
(FINANCE OFFICER)

Finance Officer
Tezpur University

Utilisation Certificate
(for the financial year ending **02 September 2017**)
From **01/04/2017** to **02/09/2017**

(Rs. in Lakhs)

1. Title of the Project/Scheme: **"Studies on the efficacy of flavonoid and nonflavonoid polyphenols against chronic inflammation induced disease pathogenesis"**
2. Name of the Organization: **Tezpur University, Assam**
3. Principal Investigator: **Dr. Rupak Mukhopadhyay**
4. Deptt. of Biotechnology sanction order No. & date of sanctioning the project: **BT/469/NE/TBP/2013 dt 03 March, 2014**
5. Amount brought forward from the previous financial year quoting DBT letter No. & date in which the authority to carry forward the said amount was given: **Rs. 7.35344 Lakhs**
6. Amount received from DBT during the financial year (*please give No. and dates of sanction orders showing the amounts paid*): **NA**
7. Other receipts/interest earned, if any, on the DBT grants: **NA**
8. Total amount that was available for expenditure during the financial year (Sl. Nos. 5,6 and 7): **Rs. 7.35344 Lakhs**
9. Actual expenditure (excluding commitments) incurred during the financial year (statement of expenditure is enclosed): **Rs. 7.14554 Lakhs**
10. Unspent balance refunded, if any (*Please give details of cheque No. etc.*): **NIL**
11. Balance amount available at the end of the financial year: **Rs. 0.2079 Lakhs**
12. Amount allowed to be carried forward to the next financial year vide letter No. & date: **NA**



Finance Officer
Tezpur University

1. Certified that the amount of Rs. **Rs. 7.14554 Lakhs** mentioned against col. 9 has been utilised on the project/scheme for the purpose for which it was sanctioned and that the balance of Rs. **Rs. 0.2079 Lakhs** remaining unutilized at the end of the year has been surrendered to Govt. (vide No. _____ dated _____)/will be adjusted towards the grants-in-aid payable during the next year.
2. Certified that I have satisfied myself that the conditions on which the grants-in-aid was sanctioned have been duly fulfilled/are being fulfilled and that I have exercised the following checks to see that the money was actually utilised for the purpose for which it was sanctioned.

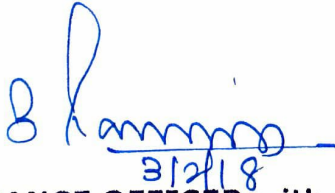
Kinds of checks exercised:

1. (Cash Book)
2. (Ledgers)
3. (Vouchers)
4. (Bank Statements)
- 5.



(Signature of PROJECT INVESTIGATOR with Stamp)

Dr.RUPAK MUKHOPADHYAY
Assistant Professor
Department of M B B T
TEZPUR UNIVERSITY
Tezpur Assam 781006


3/2/18

(Signature of FINANCE OFFICER with Stamp)

Finance Officer
Tezpur University



(Signature of HEAD OF THE INSTITUTE with Stamp)

Registrar
Tezpur University

(To be countersigned by the DBT Officer-in-charge)